The role of acetic acid in degradation of polymers for photovoltaic modules

Mihaljević, Antonia

SVEUČILIŠTE U ZAGREBU

FAKULTET KEMIJSKOG INŽENJERSTVA I TEHNOLOGIJE

SVEUČILIŠNI DIPLOMSKI STUDIJ

Antonia Mihaljević

DIPLOMSKI RAD

Zagreb, rujan 2015.

SVEUČILIŠTE U ZAGREBU

FAKULTET KEMIJSKOG INŽENJERSTVA I TEHNOLOGIJE

SVEUČILIŠNI DIPLOMSKI STUDIJ

Antonia Mihaljević

THE ROLE OF ACETIC ACID IN DEGRADATION OF POLYMERS FOR PHOTOVOLTAIC MODULES

ULOGA OCTENE KISELINE U RAZGRADNJI POLIMERA ZA FOTONAPONSKE (PV) MODULE

DIPLOMSKI RAD

Voditeljica rada: Emi GovorčinBajsić, prof. dr. sc.

Članovi ispitnog povjerenstva:

Prof. dr. sc. Emi Govorčin Bajsić,FKIT

Prof. dr. sc. Zlata Hrnjak Murgić,FKIT

Doc. dr. sc. Marijana Kraljić Roković,FKIT

Zagreb, rujan 2014.

Acknowledgements

This research work was performed at the Polymer Competence Center Leoben (PCCL) within the project "EVANetz" (FFG Nr. 838650, e!mission, Klima- und Energiefonds) in cooperation with the Chair of Materials Science and Testing of Plastics at the University of Leoben. The PCCL is funded by the Austrian Government and the State Governments of Styria and Upper Austria.

First of all I would like to thank Dr.Gernot Oreski for giving me opportunity to participate in this project and to do my master thesis under his supervision. His patience, supportive attitude, knowledge and advices helped me a lot through all process. Many thanks to my mentor dr.sc. Emi Govorčin – Bajsić for accepting this kind of cooperation. Also, I would like to thank DI Bettina Hirschmann for all advices and constructive conservations we had. Many thanks to DI Kathrin Bergmann and DI Katharina Bruckmoser for their help and advices..

Most of all I would like to thank my family and my boyfriend for all support they provided me during all these years. Their love and understanding was and always will be encouraging.

Abstract

The main aim of this thesis was to measure the acetic acid permeation rates of various backsheet films at different temperature levels. At the moment, the dominating encapsulation material for PV modules is chemically cross-linked ethylene vinyl acetate copolymer (EVA). Besides the time and energy consuming module lamination process, the major drawback of EVA is the formation of corrosive degradation products like acetic acid. Acetic acid, which is formed during oxidation of ethylene vinyl acetate (EVA), leads to corrosion of the metal parts in a PV module, PID effect and to loss of adhesion and subsequent delamination of the PV module components. Furthermore, the formed acetic acid accelerates the oxidation process of EVA. Additionally, the degradation of the cell and the cell interconnections can be accelerated by degradation co-products of the encapsulant or by molecules and substances which diffused through the encapsulant. In this thesis the influence of temperature was investigated and permeation rates were measured by gravimetry. The samples were cut to size in order to fit in an open screw cup. Vials were filled with acetic acid and closed with the previously prepared screw cup containing the sample, which now functions as a membrane. The weight loss over 30 days was followed gravimetrically at 25°C, 65°C and 85°C. Gravimetric analysis showed significant differences in the permeation behavior. The lowest permeation rates were found for laminates containing a polyester (PET) core layer and fluorpolymers. Co-extruded backsheets based on polyamides and polyolefines exhibited values which were up to 110 times higher than for laminates containing PET. According to the Arrhenius equation, an increase in temperature resulted in higher permeation rates. Higher concentration of acetic acid was found in minimodules with backsheets with lower AATR due to autocatalytic effect of retained acetic acid on the interface EVA/backsheet. Degradation of EVA due to acetic acid was investigated via spectroscopic methods (UV/Vis/NIR and Raman spectroscopy). Results showed that lower degradation was observed in minimodules combined with backsheets with high AATR.

Keywords: PV module, EVA, acetic acid, permeation, degradation

Sažetak

Cilj ovog rada bio je izmjeriti stupanj prijenosa octene kiseline kroz različite polimerne filmove koji se koriste kao stražnji zaštitni sloj pri različitim temperaturama. Etilen vinil - acetat (EVA) trenutno je najdominantniji materijal koji se koristi kao prednji zaštitni sloj (omotač) u fotonaponskim modulima. Jedan od većih nedostatak EVA je formiranje produkata s korozivnim djelovanjem poput octene kiseline. Octena kiselina, koja nastaje tijekom oksidacije etilen vinil - acetata (EVA) dovodi do korozije metalnih dijelova fotonaponskog modula, PID efektu te smanjenju adhezije što uzrokuje delaminiciju komponenata fotonaposnkog modula. Dobivena octena kiselina ima autokatalitičko djelovanje te ubrzava oksidacijske procese EVA. Degradacija solarne ćelije i spojnih dijelova može biti ubrzana razgradnim produktima koji difundiraju kroz prednji zaštitni sloj. U radu je termogravimetrijskom tehnikom istražen utjecaj temperature na stupanj prijenosa octene kiseline. Uzorci polimernih filmova izrezani su te umetnuti u prethodno pripremljene čepove kojima su zatvorene bočice s octenom kiselinom. Na taj način čepovi su funkcionirali kao membrana. Bočice su smještene na sobnu temperaturu te u peći na 65 i 85°C. Tijekom 30 dana praćen je gubitak mase bočica s octenom kiselinom. Termogravimetrijska analiza pokazala je značajnu razliku u permeaciji octene kiseline kroz različite materijale. Najniži stupanj prijenosa octene kiseline zabilježen je kod laminata s poliesterskim slojem (PET) kao središnjim slojem te kod fluoropolimera. Stražnji zaštitni slojevi od poliamida (PA) i poliolefina pokazali su vrijednosti čak 110 puta veće nego laminati s poliesterskim (PET) slojem. Prema Arrheniusovoj jednadžbi, povećanjem temperature došlo je i do povećanja prijenosa octene kiseline. Veća koncentracija octene kiseline uočena je kod minimodula koji imaju niži stupanj prijenosa octene kiseline (AATR) kao posljedica autokatalitičkog djelovanja octene kiseline koja se zadržala na međupovršini EVA/stražnji zaštitni sloj. Razgradnja etilen vinil - acetata (EVA) istražena je spektroskopskim metodama (UV/Vis/NIR i Raman). Rezultati su pokazali kako se minimoduli kombinirani sa stražnjim slojem koji ima visoki AATR manje razgrađuju u odnosu na one s niskim AATR vrijednostima.

Ključne riječi: Fotonaponski moduli, EVA, octena kiselina, permeacija, razgradnja

Contents

1. Introduction

The crystalline silicone solar cells, which are providing the highest energy conversion efficiencies, are still the most employed type of solar cells in PV industry. The most important part in a PV module is the cell. Since c-Si photovoltaic cells are thin and brittle they have to be protected from the weather from front and back. Due to their economic and performance advantages, polymers within PV modules are employed as encapsulation and backsheet material. Encapsulation plays an important role in the PV modules, whose main function is to serve as adhesive and protect cells against environmental factors. Some of the requirements for encapsulation are low modulus, high damping capacity and optical transparency. Being the most capable to fulfill these requirements, ethylene – vinyl acetate (EVA) has become the most popular encapsulation material for PV industry. Polymeric backsheet materials, on the other hand, are commonly used in PV modules for physical protection, enhanced encapsulation, light reflection, electrical insulation and aesthetic purposes. They are multi layer laminates usually containing PET and fluoropolymer layers. Although PV modules have to have a service lifetime of more than 20 years, exposure to environmental conditions (UV, O_2, humidity, dust, hail) leads to unintended degradation effects like: yellowing, corrosion and potential induced degradation (PID). All of these processes are enhanced by permeation properties of backsheets and encapsulation materials. When exposed to environmental conditions, EVA tends to degrade by mechanism of Norrish I and II reactions, producing ketones, polyenes and acetic acid as byproducts. Formation of acetic acid within EVA and its permeation through backsheet layer represents the major problem. It is well known that acetic acid has strong influence on long term reliability of PV modules, i.e. on yellowing of EVA, corrosion of metallization and PID effect. There is assumption that more breathable backsheets would support diffusing out of acetic acid. Therefore it is important to combine EVA with backsheets that have great permeation properties. The influence of degree of crosslinking on thermal stability of EVA was examined within this work. Also, transmission rates of acetic acid for different materials were calculated. In order to support assumption that combination of backsheet and EVA influences degradation of PV modules, minimodules consisting of EVA and different backsheets were prepared. Effect of external stresses (UV/T, DH) on formation and permeation of acetic acid (GC/MS) and its influence on degradation of minimodules (UV/Vis/NIR and Raman spectroscopy) was investigated in this work.

2. General part

2.1. Photovoltaic module

Photovoltaic (PV) modules are solid-devices that convert sunlight, the most abundant energy source on the planet, directly into electricity without an intervening heat engine or rotating equipment. [1]

Bell Laboratory fabricated the first crystalline silicon solar cell in 1953, achieving 4.5% efficiency, followed in 1954 with devices up to 6% efficiency. [2] Although these solar cells were firstly used on spacecraft in early 1958, the birth of terrestrial photovoltaic industry was in the mid 1970s. Typical cell efficiencies have improved from 10% (1979) to 15% - 16% today. [3] Solar power keeps attracting the largest number of new investments in the field of renewable energies (see Figure 2.1.). [4]

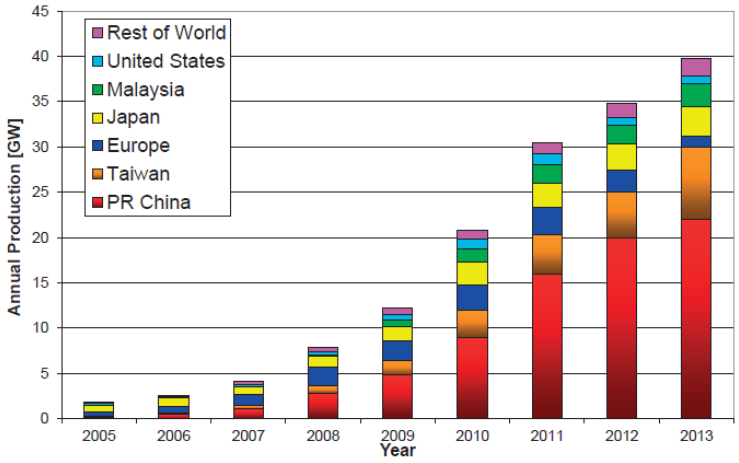

Figure 2.1. World PV cell/module production from 2005 to 2013 [4]

The most important advantage of PV modules is the production of electricity without emission of greenhouse gases or any other gases. Furthermore, silicon is safe for the environment and one of the most abundant resources on Earth representing 26% of crustal material. [2] Also, a great advantage relative to other renewable energies is the possibility of installation in a variety of places like rooftops or parking places, eased installation of additional modules and simple maintenance. Another great fact is that PV produces electricity during the afternoon when there is the highest demand and is located close to the electricity users which reduces transmission costs. [5]

2.1.1. Types of PV technology

Cells made of materials with band gap between 1 and 1.8 eV can be used efficiently in PV devices. [6] The materials most commonly used for production of PV cells are silicon (Si) and compounds of cadmium sulfide (CdS), copper sulfide (Cu_2S) and gallium arsenide (GaAs). [5]

There are many types of PV cells available today and depending on the type of light absorbing material used, the solar cell technology can be broadly divided into three groups: silicon-based technologies, compound semiconductor based technologies and other emerging technologies. [6] Also, PV cells can be divided into 3 generations: first generation are crystalline silicon solar cells, second are thin-films and third are nano-PV solar cells. [5,7] Crystalline silicon cells are most popular solar cells on the market and provide the highest energy conversion efficiencies. [2] But due to high cost of crystalline silicon wafers, cheaper materials are being explored. Crystalline cells are more efficient, while thin-film modules tend to have higher yield, especially at high temperatures. [5] The choice between crystalline or thin-film PV modules depends greatly on climate and space.

Monocrystalline silicon cells are made from pure monocrystalline silicon which has a single continuous crystal lattice structure with almost no defects and impurities, see Figure 2.2a. The main advantage is its high efficiency (typically around 14-15%). [5] On the other hand, the manufacture process is relatively expensive, the power output decreases more rapidly with increasing cell temperature (compared to thin-films) and they are susceptible to light-induced degradation (LID). [2]

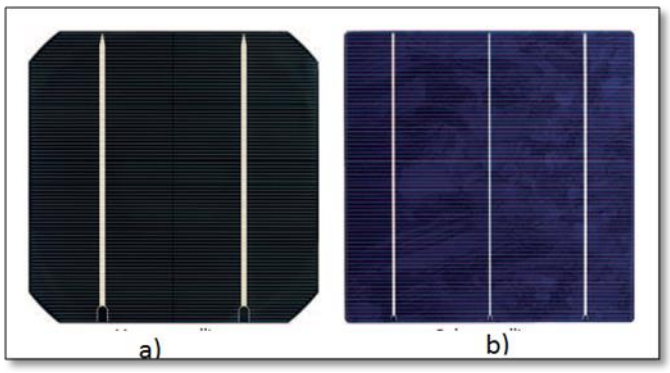

Figure 2.2.a) monocrystalline solar cell; b) polycrystalline solar cell [2]

Multicrystalline silicon cells, also known as polycrystalline silicon cells, are produced using multiple grains of monocrystalline silicon (Figure 2.2b). Since the manufacturing process of multicrystalline silicon solar cells is simpler, they are much cheaper to produce. Still, they are slightly less efficient (typical module efficiencies are around 13-15%) because of higher packing factor of the square polycrystalline cells. However, polycrystalline solar cells are currently the most widely produced cells, making about 48% of the world solar cell production. [2]

Although wafer-based technologies, mono - and multicrystalline silicon solar cells, offer great advantages such as: durability, relatively high conversion efficiency, relatively low capital costs for capacity expansion, relative maturity of its supply chain, thin-film technology still uses much less material for production of solar cells. [8, 3]

One of the most used *thin-film solar cells* are amorphous silicon (a-Si) solar cells, cadmiumtelluride (CdTe) solar cells and copper indium gallium selenide (CIGS) solar cells. Unlike mono- and multicrystalline solar cells, the silicon atoms in amorphous silicon (a-Si) solar cells are arranged in a thin homogenous layer and absorb light more effectively than crystalline silicon cell. Regarding absorption, a-Si silicon cells are more capable to absorb blue wavelengths of light that are encountered during cloudy conditions. [2] Other advantages are low manufacturing cost, high energy production per rated power capacity and a-Si silicon cells are the least impacted by heat. Maybe the greatest advantage of a-Si is possibility of deposition on a wide range of substrates (rigid or flexible) which leads to variety of shapes suitable for different applications, such as roof tiles. Still, the efficiency of a-Si modules is only 6-7%.

Although CdTe and CIGS thin-films offer much higher efficiency around 10-13% and are lightweight, it is not that likely that their production and usage will prevail over silicon based solar cells because of the low concentration of these elements on Earth which makes their production much more expensive. [9, 5]

2.1.2. PV module setup

A general module constitution is shown at Figure 2.3. below. It can be seen that PV module consists of four different materials: glass, metals, polymers and semiconductor. These materials are used for the front cover (glass), the frame and interconnectors (metal, usually aluminum), as encapsulation material (polymer – EVA, PBV…) and as backsheet (polymer or glass). [10]

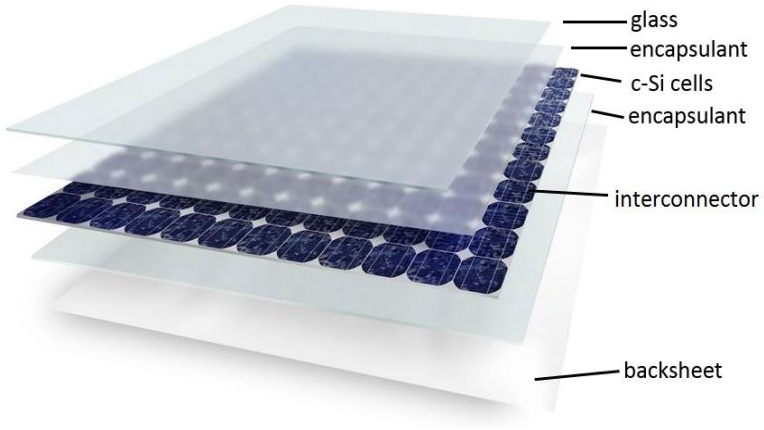

Figure 2.3. Design of photovoltaic module [11]

The most important part in a PV module is the cell. All other components are just needed for the transport of the produced electricity, to protect the cell from environmental influences and to give electrical insulation due to safety issues. [11] Since c-Si photovoltaic cells are thin and brittle they have to be protected from the weather from front and back. The most common used material for front protection is rolled sheet glass (thickness around 3 mm) which is typically tempered and has low iron content. [12] It provides not only protection but also mechanical rigidity, impact resistance, optical transparency, electrical isolation of the solar cell circuit and outdoor weatherability. [12]

Since polymeric encapsulant that is placed under the glass can easily degrade under extended exposure to UV light, a small amount of the element cerium (Ce) is added to glass formulations used in PV module in order to absorb the short wavelengths and to prevent UV degradation. [12] Not only glass, but also UV-stabilized plastic sheets made of flouropolymers like: ETFE or FEP, can also be used as front cover.

Different metals (aluminum alloys, stainless steel, copper, soldering agents…) are used for frames, interconnectors, cables, fingers and grids (Figure 2.4.). [12] To transport the electricity from the solar cells, bus-bars are needed. Those are copper ribbons that are completely covered with solder material which is typical a lead Pb-free or Pb containing tin. The main purpose of solder material is to contact the bus-bars under heat to the metallization surface of the solar cells (via soldering). [11] Finally, electrical current from the gridlines is collected by bus-bars and transported on the back of the neighboring solar cell, and via these paths to the junction box on the upper back of PV module.

The encapsulant is bonding or laminating the multiple layers of PV module together, protecting PVmodule from different kinds of weathering conditions. [6] This is a critical

component of PV module which should provide structural support, optical coupling, electrical isolation, physical isolation/protection and thermal conduction of solar cell assembly. [13] Additional encapsulant characteristics must include high optical transmittance, good adhesion to different module materials, adequate mechanical compliance to accommodate stresses induced by differences in thermal expansion coefficients between glass and cells and good dielectric properties (electrical insulation). [12]

2.1.3. Polymeric materials in PV modules

The reasons why polymeric materials are incorporated in PV modules are their economic and performance advantages. They are typically of lighter weight than other materials, relatively cheap and easy to process. [13, 14] Polymers in PV modules are used in the form of encapsulants and backsheets. EVA or silicones are usually used as encapsulants. The encapsulant is exposed to environmental conditions and therefore it needs to meet the requirements for encapsulation materials to prevent its fast degradation. The encapsulant should be especially stabilized with different UV absorbers because it easily degrades under UV radiation resulting in discoloration of the material and other degradation mechanisms.

The backsheet is usually a laminate of polyethyleneterephthalate (PET) and fluoropolymers (PVF, PVDF, THV, ECTFE). PET is known for its great barrier properties and therefore is usually used as barrier layer. Fluoropolymers provide excellent optical and mechanical properties and have extraordinary stability against UV radiation [15] and are used as outer and inner layer.

Although being lightweight, cheap and easily available, polymers are prone to degradation under extended exposure to environmental conditions (UV, humidity and temperature) and play a critical role in determining the long term performance of solar panels. [16]

2.1.3.1. Backsheets

Polymeric backsheet materials are commonly used in PV modules for physical protection, enhanced encapsulation, light reflection, electrical insulation and aesthetic purposes. [16] Backsheets for PV modules have several critical properties which must be maintained over the product life-time which include mechanical, optical, thermal, electrical and chemical properties. Nevertheless, mechanical integrity, adhesion and color stability seem to be most critical properties to consider. [17] Requirements for backsheets are low cost, low water absorption and permeability, high resistance to UV degradation and thermal oxidation, chemical inertness and good adhesion to encapsulation material. [18]

A backsheet typically includes three layers of laminated polymer films with each layer of the structure having specific functional requirements. The main reasons for the use of multi-layer build-ups are either the combination of required properties, which cannot be achieved by one material alone, cost effectiveness, but also consecutive processing steps. [18] Each of these layers is exposed to a different set of environmental stresses in outdoor exposure and the durability of each layer contributes to its individual performance as well as the performance of the backsheet as a whole. [17]

The outer layer (air facing layer) provides protection for other layers within the backsheet structure and to other components within the silicon module structure. Since the outer layer of the backsheet is directly exposed to the environment (UV radiation, moisture, condensation, mechanical stresses) it has weathering and durability requirements. [19] Also, during processing the outer layer needs to be tough enough to withstand the lamination process where temperatures up to 170°C for several minutes are common. [19, 16] Therefore, the outer layer is usually polyamide (PA), polyethylene terephtalate (PET) or flour-containing material e.g. polyvinyl fluoride (PVF). In most cases, backsheets exhibit a symmetrical construction with identical polymers used for the inner and the outer protection layer varying only in the amount and type of stabilizers added. [20]

The middle layer, or the central core layer, typically provides mechanical properties, electrical insulation and barrier properties. [19, 20] It is important that this layer maintains adhesion to the other layers in the backsheet and it is resistant to the typical temperatures and transmitted UV light from the inner and outer layers. It is often made of polyethyleneterephtalate (PET). To improve the barrier properties, usually an additional alumina or aluminum layer is used, but thin silicon oxide layers have also been applied. [21]

The inner layer is in contact with the encapsulant and is expected to have durable adhesion and chemical compatibility with encapsulant. Also, it needs to be stable to the direct solar exposure filtered through the glass and encapsulant layers. [17]

In commercial use, multilayered backsheet structure usually consists of polyvinyl fluoride (PVF) and polyester (PET) that are used to provide a durable package with an established long-lived performance in the field. [22]

Although PVF film complies requirements for PV applications, recently other fluoropolymer and non-fluoropolymer films have been used in PV modules as backsheets, such as: polyvinylidene fluoride (PVDF) or tetrafluoroterpolymer (THV). Among non-fluoropolymer films most employed are UV-stabilized PET and polyamide (PA). [17, 23]

The new developed layers are based on composites of different polymers [23], so two basic structures are typically found: fluoropolymer/PET/fluoropolymer structures and fluoropolymer/PET/adhesion layer (for example TPE). [17]

Due to the multi layer buildup of PV encapsulation, aging of the materials can occur at the surface, in the bulk of single layers or within the interfaces of layers, which are usually adhesively bonded. [21]

2.1.3.2. Encapsulants

Since PV cells are brittle, they have to be protected from weather conditions during operation in the field. So, encapsulation material needs to provide not only mechanical strength but also protection from hazardous environmental conditions (rain, hail, dust, salt spray, birds) and physical and electrical isolation of the solar cells and circuit components. [6, 13]

The characteristics and requirements for the encapsulating material in PV modules are listed in Table 2.1. [13 S. 107]

Table 2.1. Characteristics and requirements for the encapsulating material in PV modules

Characteristic	**Specifications or requirement**
Glass transition temperature (Tg)	< -40°C (winter in deserts)
Total hemispherical light transmission through 20-mm-thick film integrated over the wavelength range from 400 nm to 1100 nm	> 90% of incident
Hydrolysis	None at 80°C, 100% RH
Water absorption	< 0.5 wt% at 20°C/100% RH
Resistance to thermal oxidation	Stable up to 85°C
Mechanical creep	None at 90°C
Tensile modulus as measured by the initial slope of a stress-strain curve	< 20.7 MPa (< 3000 psi) at 25°C
Fabrication temperature	≤ 170°C for either lamination or liquid pottant system
Fabrication pressure for lamination pottants	≤ 1 atm
Chemical inertness	No reaction with embedded Cu coupons at 90°C
UV absorption degradation	None at wavelength > 350 nm
Hazing or clouding	None at 80°C, 100% RH
Minimum thickness on either side of solar cells in fabricated modules	0.152 mm (0.006”)
Odor, human hazards (toxicity)	None

Because of these demanding requirements, only a few polymers are suitable for encapsulation of PV modules: silicones, EVA, polyethylene and polyethylene copolymers. [14] Structure of silicone polymer is shown in Figure 2.4. below. Silicone fluids, resins and elastomers have been in use for over 50 years. The silicones are nonconductors of either heat or electricity,

have good resistance to oxidation, ozone, UV-radiation (weatherability) and are generally inert. Also, they have a constant property profile of tensile, modulus and viscosity values over a broad temperature range from 13 to 166°C. Furthermore, they have a low glass transition temperature (Tg) of -125°C. [24] Despite that, they perfectly meet requirements for encapsulating material in PV modules and their price is still much higher than the price of EVA for commercial use. [14]

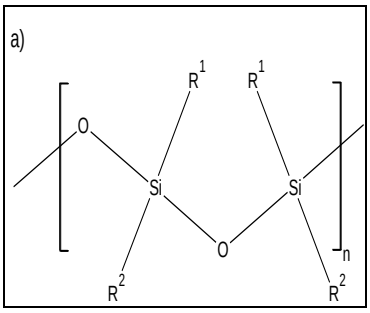

Figure 2.4. Structure of silicones

The reason why the EVA is most employed encapsulation material over other aforementioned materials is the fact that it perfectly meets requirements (Table 2.1.) for encapsulation materials with relatively low price of raw material. Furthermore, the EVA film can be produced from an extrusion process before lamination with the silicon solar cell and the glass substrate in a vacuum bag typically at a temperature of less than 170°C. Beside easy production, EVA offers excellent optical clarity and hydrophobicity. [14, 25] Another advantage in production of EVA is the possibility of controlling gel content and tensile modulus of EVA by adjustment of the compounding formulation.

2.2. Degradation mechanisms in PV module related to EVA/acetic acid

When operating in the field, PV modules are exposed to different environmental conditions such as solar and UV irradiation, rain, hail, temperature changes, dust, salt, humidity, see Figure 2.5.

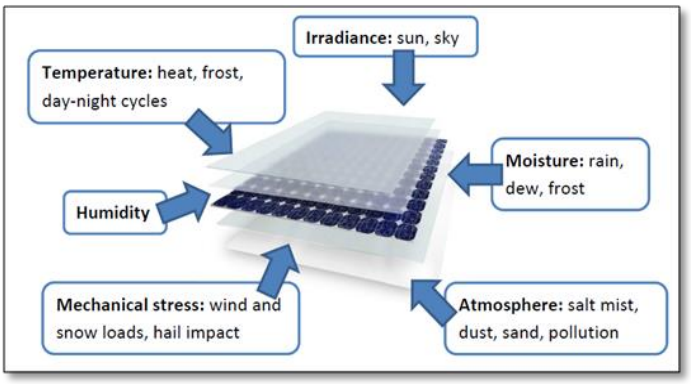

Figure 2.5. Various environmental impacts on a PV module during application [11]

All stress factors are singular stress parameters, but they are often present and active in different combinations. These combinations have a higher damage potential than the sum of the single tests. [10]

The long-term deterioration to EVA during its service life also involves interactions between oxygen, heat, moisture absorption and UV radiation from sunlight. [26] Since EVA is the most widely used encapsulation material, many studies were conducted in order to understand degradation mechanisms of EVA under these different environmental conditions. [27]

One of the most observed degradation mechanism is the yellowing of EVA, i.e. changing color from yellow to brown (see Figure 2.6.) which affects performance and power conversion of a PV module. (13,14, 28-33] Although yellowing can occur in backsheets too, it is reported to have no influence on the electrical performance of the modules. However, it obviously indicates polymer degradation. [34] It was assumed that the formation of conjugated double bonds (polyenes), ketones and lactones that are formed during the formation of acetic acid via Norrish II reactions in the polymer chain causes the discoloration of EVA. [35] These degradation by-products are assumed to be chromophores that are absorbing visible light and therefore are responsible for yellowing of EVA. Since EVA is usually formulated with UV absorbers, antioxidants and crosslinking agents, some authors investigated influence of the EVA formulation on its discoloration. So Klemchuk et al. found that yellowing is a consequence of interactions between peroxide curing agent and the UV absorbers or phosphite compounds. [36] Peike et al. investigated effect of different additive formulations on discoloration of EVA. Experiments showed that highly stabilized EVA films showed higher discoloration rates. Therefore, it is claimed that the stabilizers resulted in the formation of lumophores and chromophores. [29]

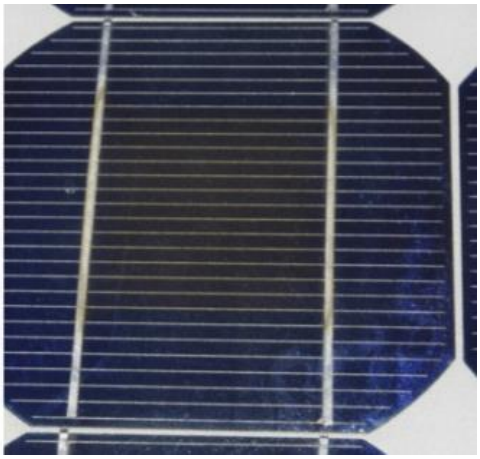

Figure 2.6. Slightly browned EVA in the center of a multicrystalline Si-cell [11]

Delamination can occur between the boundary surfaces of glass to encapsulant, encapsulant to solar cell, encapsulant to backsheet and within the layers of the backsheet (Figure 2.7.) [34,37]

Figure 2.7. Delamination of backsheet [11]

It is a consequence of reduction in adhesion between different layers (cell, encapsulant, backsheet and glass) due to non homogeneous temperature in the laminator during production, aged encapsulant and use of many layers. [38] When delamination occurs between the encapsulant and the glass or cell surface, light will be reflected on the boundaries and therefore not able to reach the solar cell. Delaminations within the layers of the backsheets are caused by adhesive degradation via hydrolysis. Therefore, delamination within the polymeric layers can give new pathways for water vapor and acetic acid which can lead to corrosion of the solar cell surface (ARC) and interconnectors as well as to degradation in the polymer like hydrolysis or photo-oxidation. [11]

Another often discussed issue is the production of acetic acid via thermal or photo-thermal degradation of EVA. [13,25,28,32,39] The acetic acid has corrosive effect on interconnectors and cell metallization which leads to an increased series resistance and therefore losses in module performance. [25,32] Due to long diffusion paths from encapsulant to the backsheet, acetic acid can accumulate in front of the solar cells and lower the pH value which leads to even faster corrosion. [39] Not only that it accelerates corrosion, but it also has an autocatalytic effect on the EVA yellowing. [13,40]

Another cause of failure in c-Si modules is the potential induced degradation (PID) effect. Therein high system voltages cause leakage currents through the glass cover and the encapsulation material. The resulting electrical potential between frame and cells causes a detrimental effect on power output. The encapsulant can also influence the PID effect. For example, EVAs with high volume resistivity guarantee strong PID resistance. But volume resistivity can be affected by composition of EVA (lower VA ratio enhances volume resistivity) and temperature (high temperature reduces resistivity of EVA and seem to be a critical factor). The PID effect can also be enhanced by acetic acid which eases the transport of Na^+ from glass to the cells. [11]

From all of the above mentioned, it can be seen that acetic acid has a great role in degradation of PV module. Regarding the lifetime of PV modules, it is important to understand mechanism of acetic acid formation within EVA and its migration through backsheet.

2.2.1.Degradation of PV module regarding to permeation

The permeability coefficient or, simply, permeability is the amount of substance passing through a polymer film of unit thickness, per unit area, per second and at a unit pressure difference. [41,42]

$$P = (N_A L)/(p_2 - p_1) \qquad (2.1.)$$

Hence, permeability has dimensions of quantity of penetrant (either mass or moles) times thickness divided by area, time and pressure. Several units are used, but the most preferred is the SI unit (mol m)/(m^2 s Pa). [41] The steady-state transport properties of water vapor in polymers are characterized by the water vapor transmission rate (WVTR) and for oxygen by the oxygen transmission rate (OTR). [11,41] It is established to use the unit g m^{-2} day^{-1} for VWTR and cm^3 m^{-2} day^{-1} bar^{-1} in case of OTR. Both rates in this form are dependent on the layer thickness and therefore for each film specific. Hence, thickness of layer must be given

when representing results. In some cases also different units are used, dependent on the measurement technique. [11]

2.2.2. Mechanism of penetrant transport in polymeric materials – Free Volume

Penetrant transport through polymers is described by „solution-diffusion model“ which describes permeation through a flat sheet or film. According to that model, permeation is conducted in three steps: dissolution of molecules in the polymer following absorption at the surface, diffusion of molecules through material, driven by concentration gradients and desorption from the surface of the material. [43] The rate limiting process in this process is diffusion of penetrant through the film that typically follows Fick´s law:

$$N_A = -D(\mathrm{d}C/\mathrm{d}x) \qquad (2.2.)$$

where the D is the diffusion coefficient for the penetrant in the polymer and dC/dx is the local concentration gradient of the penetrant. [41] Therefore permeation rates are defined as product of the sorption coefficient and the diffusion coefficient (P=D*S). The transport of the molecules occurs until there is an equal concentration on both sides of the separating material. [11]

The migration of the penetrant can be visualized as a sequence of unit diffusion steps or jumps during which the particle passes over a potential barrier separating one position from the next. This jumps involves a cooperative rearrangement of the penetrant molecule and its surrounding polymer chain segments. Hence, penetrant molecule and its surrounding chain segments may share common volume before and after the diffusion jump. [44] This volume is known as *free volume* or *fractional free volume* (FFV) and occurs as a consequence of packing inefficiencies and polymer chains molecular motions. [41]

Free volume is an intrinsic property of the polymer matrix. [43] This is the fraction of volume in a polymer that is available to assist in penetrant transport and does not include volume occupied by polymer molecules and volume in the polymer matrix that is otherwise unavailable for penetrant transport. [41] Free volume can be thought of as an extremely small-scale porosity. But free volume pores are dynamic and transient in nature since the size of any individual free volume „pore“ depends on the vibrations and translations of the surrounding polymer chains. The translation of the polymer chains can open/close “pores“ and open/close channels between pores (see Figure 2.8.), providing „pathways” for diffusion jumps, respectively. [41,43]

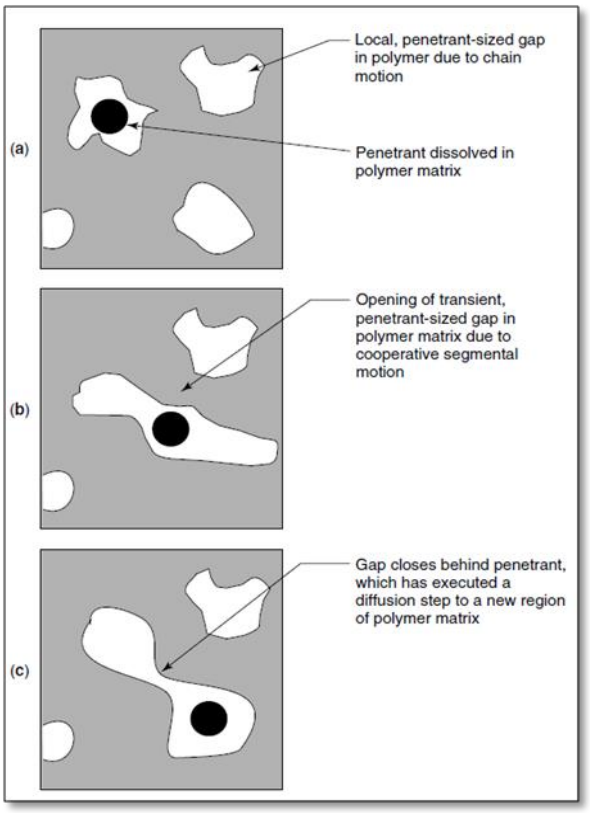

Figure 2.8. Schematic depicting mechanism of penetrant transport in polymers [41]

In Figure 2.8. it can be seen that local polymer segmental motion has opened a connecting channel between two free volume elements and in that way provided space for Brownian motion of polymer segments. [41] During motions, polymer segments form transient gaps that influences penetrant diffusion as well as concentration of free volume. Hence, it can be stated that the polymer segmental motion is the rate-controlling step in the penetrant diffusion and the diffusion is larger with higher FFV. But also it must be clear that the rate of production of gaps of sufficient size to accommodate penetrant molecules decreases with increasing size of the penetrant. [41,43]

Free volume depends on the crystallinity, physical ageing and molecular orientation of the polymer.

2.2.3. Factors affecting permeability – Temperature

Factors that are affecting permeability are:

- free volume (FFV)
- chemical structure
- degree of crysatallinity
- chain orientation
- penetrant concentration
- porosity and voids
- fillers
- mechanical stress and strain
- molecule sizes and
- temperature

The permeation process is strongly temperature controlled and can be determined by performing measurements at different temperatures. Temperature has an effect on the permeability and diffusion properties of small molecules in the polymers. As the temperature increases, the mobility of the molecular chains increases and therefore thermal expansion leads to reduced density. As a consequence, the FFV in the system will increase which leads to an increased solubility. [43]

The temperature dependence of permeability and diffusivity are usually modeled using Arrhenius equations of the following forms:

$$P=P_0\exp(-E_P/RT) \quad (2.3.)$$

$$D=D_0\exp(-E_D/RT) \quad (2.4.)$$

where E_P and E_D are activation energies for permeation and diffusion, and P_0 and D_0 are temperature independent permeation/diffusion coefficients, R gas constant and T is temperature (K). [11,41] The temperature dependence is specific for every polymer. Therefore permeation results should always indicate at which temperature the measurements were performed. [11]

According to Equation 2.4. activation energy E_A can be calculated. The activation energy is a constant which is specific for the respective process and, in case of permeation, describes the acceleration of the permeation by temperature. Therefore, the higher E_A the bigger is the acceleration of mass transport with increasing temperature. [45]

Temperature also affects solubility of penetrant, which is described in the following equation:

$$S=S_0\exp(-\Delta H_S/RT) \quad (2.5.)$$

where the coefficient S is the solubility parameter, S_0 preexponential factor and ΔH_S is the heat of sorption of penetrant in the polymer. [43] Since steady-state permeability is the product of diffusivity and solubility, the activation energy of permeation can be defined as the sum of activation energy of diffusion and the heat of sorption, following equation:

$$E_P = E_D + \Delta H_S \quad (2.6.)$$

where E_P and E_D are always positive, while ΔH_S is often positive for light gases, but can be also negative for larger, more soluble penetrants. Therefore, permeability increases with increasing temperature. [41,43]

2.3. Structure and properties of EVA

Ethylene vinyl acetate (EVA) is semicrystalline copolymer consisting of polyethylene (PE) and vinyl acetate (VA) as repeating units. The PE chains are partly folded to crystals that form reversible physical crosslinks in the polymer network (Figure 2.9.). [33] Polyethylene itself is a very inexpensive polymer, but when used alone it is an opaque or translucent semicrystalline polymer with a modulus too high to protect PV modules. On the other hand, poly (vinyl-acetate) is a transparent and amorphous polymer that has glass transition temperature (Tg) around 35˚C. Hence, small amount of vinyl acetate was added to polyethylene in order to obtain highly transparent, semicrystalline polymeric material. [25]

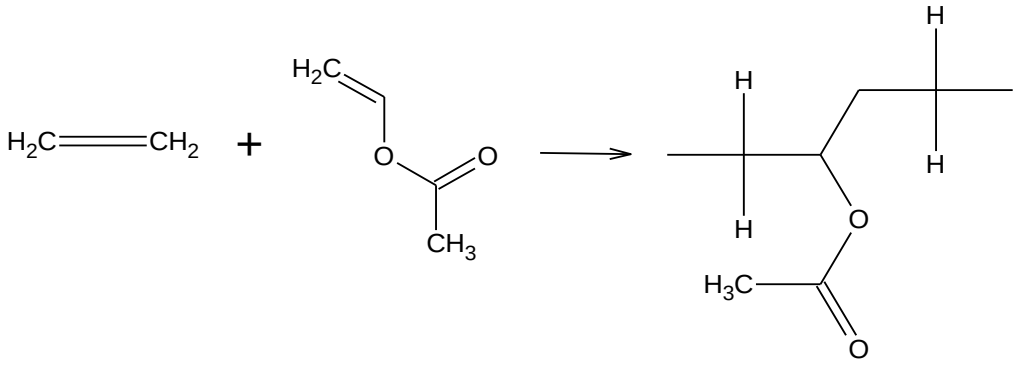

Figure 2.9. Schematic of polymerization and structure of ethylene vinyl acetate (EVA)

Polar vinyl acetate (Vac) units that are randomly dispersed in the backbone of EVA hinder the ability of the polymer to crystallize and therefore ensure excellent flexibility, fracture toughness, light-transmission properties of EVA and adhesion to other organic/inorganic materials. The properties of EVA are depending on the VA content which is ranging from 3-50 % w/w VA. Different VA content in copolymers changes EVA from thermoplasts to elastomers. [26] As a result of its excellent properties, it is used in numerous different fields such as industry of flexible packaging, footwear, cable sheeting, flexible hoses, molded automotive parts, films, etc. [46,47] Therefore, it is not surprising that ethylene-vinyl acetate copolymers represent the largest volume segment of the ethylene copolymer market. [48] Despite its excellent properties, eased production and acceptable price, application of EVA as encapsulating material has some limitations i.e. EVA is susceptible to degrade under environmental conditions (yellowing of EVA, production of acetic acid).

2.3.1. Crosslinking of EVA

Evaluating the production process of PV modules, the most time consuming step is the lamination of the modules. As the crosslinking of the EVA also takes place in this step, it appears to be highly relevant for quality and long term stability. [49] The native EVA material, which is thermoplastic, mildly opaque, soft and easily plastically deformable would not fulfill mechanical and optical requirements for encapsulant in PV modules. Still during module lamination, by crosslinking of the copolymer chains the mouldable EVA sheet is transformed into an elastomeric, highly transparent encapsulation. Therein, the formation of a loose three-dimensional polymer network is formed which is increasing thermal and mechanical stability of the (then) elastomeric material. [49,50]

Crosslinking of EVA is possible only via a radical reaction using an organic peroxide or peroxycarboxylic acid as a radical initiator, i.e. crosslinker. In this process, the crosslinker is homolytically cleaved into two radical species, which then abstract hydrogen from the EVA chain leaving active radical site which is then transferred to the methyl group. The methyl group then reacts with another active site in its vicinity creating a chemical bond between the polymer chains and transforming the initially thermoplastic EVA into a “cured” three-dimensionally crosslinked elastomer. In PV module manufacturing this radical reaction is thermally activated by thermal decomposition of the radical crosslinker around 150˚C. The degree of crosslinking is controlled by the lamination temperature, the lamination time and

the initial crosslinker concentration. [50] Also, studies of the long term characteristics of elastomers showed that degree of crosslinking has strong influence on these. [13]

2.3.2. Mechanisms of degradation of EVA

The effect of various stresses on polymeric materials in a terrestrial environment involves complex reaction processes that are usually initiated by UV radiation. [13] The degradation mechanisms are strongly dependent on the chemical and physical conditions [28] and they can be induced thermally, photo and photothermally. [13]

Generally, degradation of EVA during exposure to heat and/or UV radiation results in formation of conjugated polyenes and α,β-unsaturated carbonyl groups by many chemical reaction mechanisms including Norrish I and Norrish II type reactions. Formed polyenes are capable of absorbing visible light and are considered to be the chromophores. Accordingly, they show strong fluorescence and it is assumed that they are responsible for the yellowing of EVA. Not only conjugated polyenes, but also volatile compounds like acetic acid and hydroperoxides are formed. [13,14,27]

EVA tends to degrade by two-step degradation mechanism when heated which results in formation of acetic acid. The deacetylation mechanism occurs around 560 K by mechanism of ester pyrolysis, i.e. Norrish II mechanism, as shown on Figure 2.10.below. [28]

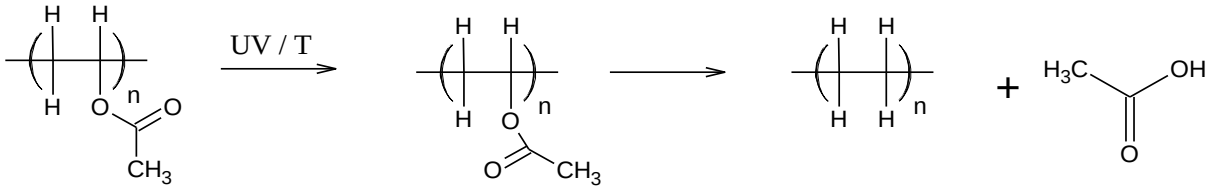

Figure 2.10. Norrish II reaction of EVA during thermo-degradation

The formation of acetic acid occurs at much lower temperature than ester pyrolysis, around 390-410 K. Further products of EVA degradation are lactones, ketones and aldehydes. [28] Lactones are formed via an intermolecular back-biting by the acetate group and evolution of methane (Figure 2.11.), while ketones are formed either via acetaldehyde evolution or hydroxide breakdown (Figure 2.12.) [26]

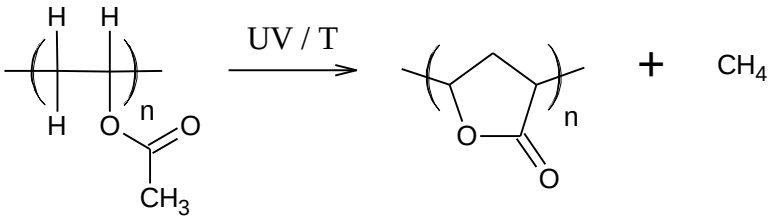

Figure 2.11. Lactones formation via back-biting process

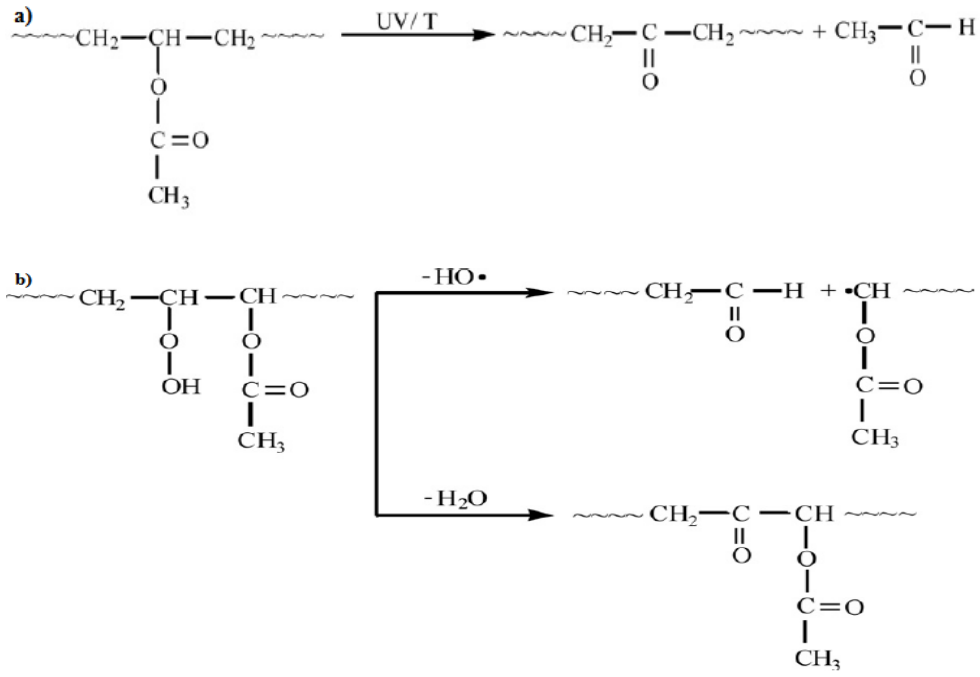

Figure 2.12. a) Ketones formation via acetaldehyde evolution; b) ketones formation via hydroperoxide breakdown [26]

The EVA formulation plays a major role in the amount of acetic acid produced. Since it is a common agent in polymer processing, acetic acid may also be found in acetic acid free encapsulants. [11] Also, it is observed that content of VA blocks has influence on degradation of EVA. [13,26,28] A high vinyl acetate content of the copolymer enhances the hydrophilic character of EVA which provides higher solubility of acetic acid in EVA and leads to faster degradation [28] i.e. acetic acid acts as autocatalyst enhancing further production of acetic acid and therefore higher degradation. Also, other degradation by-products (polyenes, ketones, lactones, acetic acid) may accelerate further degradation.

2.4. Influence of combination of encapsulant and backsheets on degradation of PV modules

Permeates like water vapor, acetic acid and oxygen are reaction partners in degradation processes inside of PV modules. [32] The ingress of such gases is governed by the permeation properties of the polymeric backsheets or encapsulation materials used. [51] Newer approaches correlate the permeation properties of backsheets with the yellowing of EVA (or other encapsulants). [11] Not only the yellowing of encapsulant, but also other mechanisms of degradation of PV like corrosion, delamination and PID effect are connected with permeation properties of backsheets. Water vapor is known to have critical impact on various degradation mechanisms of PV modules especially on corrosion of metal, cell parts and solar cell surface and encapsulant decomposition via hydrolysis. However, some level of water vapor transport could be desirable and effective in allowing water to leave the PV module and thus reducing corrosion rates. [17] Oxygen, on the other hand, contributes to chemical processes like photo- and thermooxidation. [11,13] Acetic acid, which is formed in EVA during aging, has great impact on aging mechanisms like yellowing of EVA, PID effect, corrosion of metal parts and delamination. Furthermore, the metallization corrosion leads to an increased series resistance and therefore losses in module performance.

Some authors stated that for some encapsulation/backsheet combinations the susceptibility to degradation is much lower than to other combinations. [25,32] For that reason the influence of the laminate combination of encapsulant/backsheet was investigated under different accelerated aging conditions. [32] As observed, the permeation properties, i.e. the water vapor transmission rate (WVTR) and oxygen transmission rate (OTR), were on average higher for the encapsulants than for backsheets. [32] Therefore it is highly relevant to choose the right combination of e.g. a backsheet with high OTR with an encapsulant which leads to discoloration under UV irradiation and a backsheet with low WVTR with an encapsulant susceptible to hydrolysis. [25,32] Therefore permeation properties of backsheets are an important consideration regarding to reliability of PV modules. [32,51]

3. Characterization of samples

3.1. Thermogravimetry or Thermogravimetricanalysis (TGA)

Thermogravimetric analysis (TGA) or thermogravimetry (TG) is a technique where the mass of a polymer is measured as a function of temperature or time while the sample is subjected to a controlled temperature program in a controlled atmosphere. A purge gas flowing through the balance creates an atmosphere that can be inert, like nitrogen (N_2), argon (Ar) or helium (He); oxidizing, such as air or oxygen (O_2); or reducing, such as forming gas (8-10% hydrogen in nitrogen). Moisture content of the purge gas can vary from dry to saturated. The heart of the TG analyzer is the thermobalance (Figure 3.1.) that is capable of measuring the sample mass as a function of temperature and time. [52]

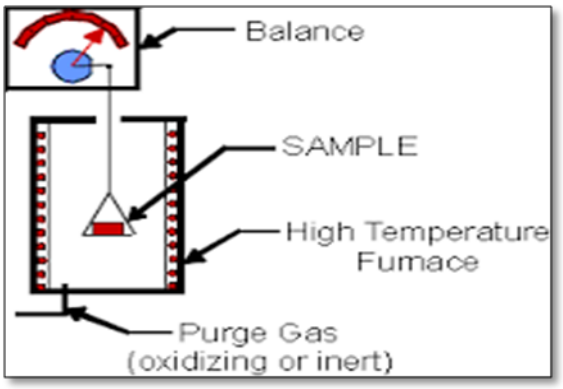

Figure 3.1. Schematic of TG analyzer [53]

Besides measuring change of mass as a function of temperature (dynamical thermogravimetry) or as a function of time (isothermal gravimetry), the instrument also measures first derivation of mass as a function of time (dm/dt). As a result of measurements, typical curve is obtained (see Figure 3.2.). Shape of the curve depends on the experiment conditions (heating rate), structure of material, mass of material and atmosphere.

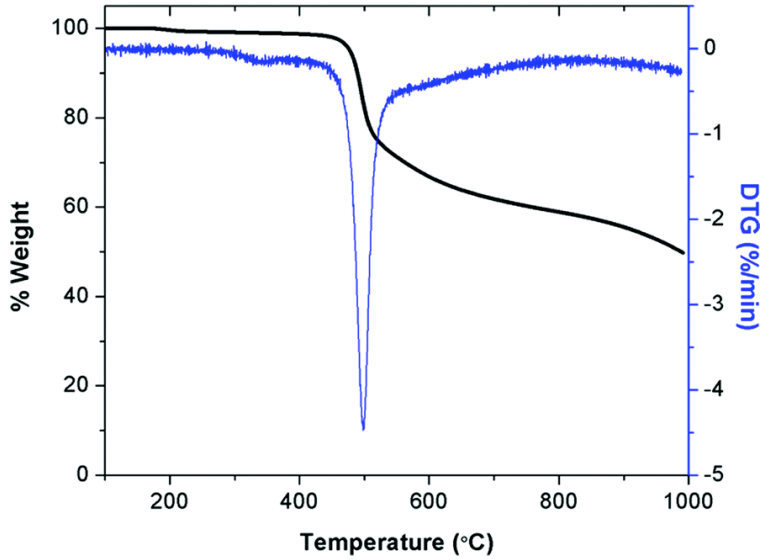

Figure 3.2. TGA and DTG curve [54]

Analysis of the curve exhibits information about mass loss which may be categorized as volatile compounds such as absorbed moisture, residual solvents or low-molecular-mass additives or oligomers that generally evaporate around 300°C. [52,55] Also, analysis provides information about amount of thermally degraded matter and range of temperatures of degradation, i.e. about thermal stability of material. [55]

3.2. Gas chromatography with mass spectrometry – GC-MS

Gas chromatography as a method was developed in 1950s and today is one of the basic methods in chemical analysis.

Gas chromatography (GC) is a method where separation and detection of volatile organic compounds and inorganic gases from mixture are obtained. Basis in GC method is mobile phase (gas carrier) which is usually He, N_2, H_2 or mixture of Ar and CH_4. Sample is injected in the machine via injector (manually or automatically) and carried by gas into column. Inner side of column is coated with porous material or viscous liquid in order to separate compounds in sample. Separated compounds are detected by detector. GC method uses various types of detectors depending of analyzing compound. Gas chromatography with mass spectrometry (GC-MS) is an analytical method based on separation of organic compound (GC) and detection of structure of present hydrocarbons. [56]

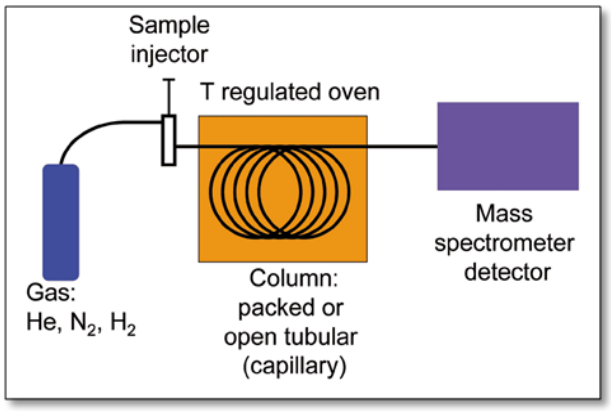

Figure 3.3. Schematic of GC-MS [57]

3.3.UV/Vis/NIR spectroscopy

Ultraviolet/Visible/Near-infrared (UV/Vis/NIR) spectroscopy is a spectroscopic method which is based on the absorption of ultraviolet and visible light of a material. For polymer characterization wavelengths between 200 and 2500 nm are used. While in IR spectroscopy absorption is based on the oscillation and rotation of the molecules, in UV/Vis/NIR spectroscopy absorption can be explained by the raise of electrons to a higher state (considering energy level).

When light beam with intensity I_0 comes into contact with sample (liquid or solid) it can be reflected with an intensity I_R, transmitted I_T, diffused, absorbed I_A, refracted or polarized. UV/Vis/NIR spectroscopy, using different kind of equipment, makes it possible to measure the different percentages of light reflected, transmitted or absorbed by the sample taking into account the various phenomena capable of producing misleading measurements (diffusion, refraction, polarization). [58] Interactions of light with a solid are depicted in Figure 3.4.

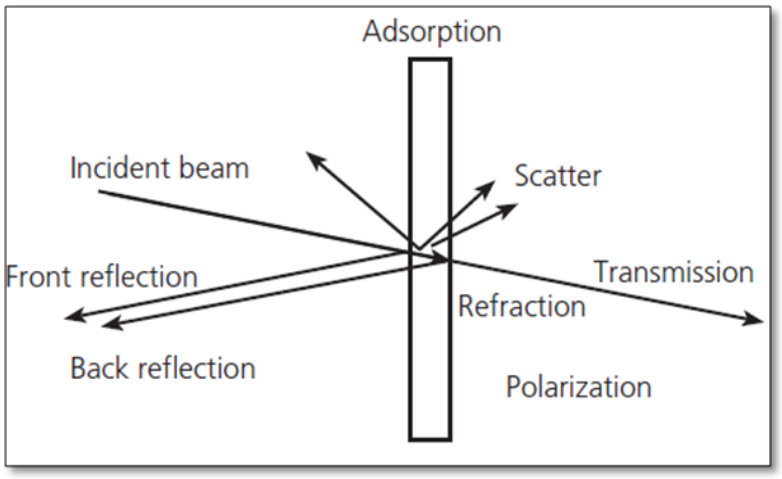

Figure 3.4. Interactions of light with solid sample [58]

3.4. Raman spectroscopy

Raman spectroscopy is technique based on the inelastic scattering of light. In contrast to infrared spectroscopy, which is more sensitive to molecular dipole moment, a change of the polarization potential, i.e. deformation of the electron cloud, is necessary for a molecule to exhibit a Raman Effect. [59]

When photons are scattered from an atom or molecules, most of them are elastically scattered. In elastic scattering, also called Rayleigh scattering, the molecule is excited to a virtual state and then relaxes to the original vibrational state by re-emitting a photon at the same frequency as the incident light. [60] In this case, the molecules "absorb" no energy from the incident radiation [60] and the frequency of the electromagnetic wave does not change. [35] On the other hand, only a very small fraction of molecules undergo inelastic scattering called Raman scattering. [60] In this case, the excited molecule relaxes to a different vibrational level, rather than to the original state. The electromagnetic wave interacts with the molecule and gets scattered with a higher or lower energy. [35]

In the Raman spectroscopy, the light source is a highly monochromatic laser light usually in the ultraviolet (UV) to the near-IR region [61] and scattered light is measured in a right angle to the incident beam. [62] The excitation radiation source is monochromatic and is much more energetic than infrared radiation. [60] Scattered photons are measured and plotted as a function of intensity over the wave number (Raman shift) and provide information about vibrational frequencies of the surface of a material (Figure 3.5.). [35]

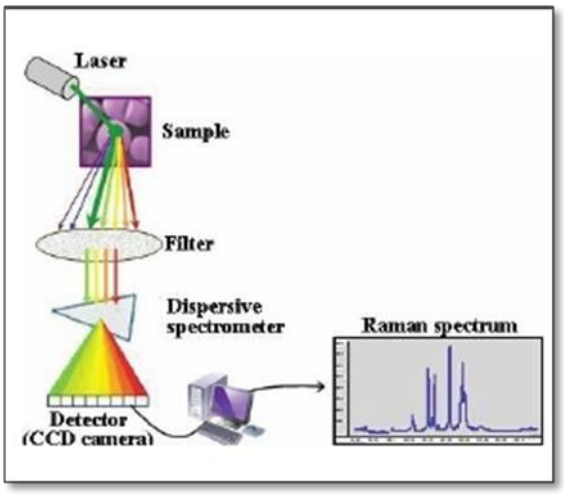

Figure 3.5. Schematic of Raman spectroscopy [63]

The intensity of the Raman scattering is proportional to change in polarization during the vibration. The use of short excitation wavelength is reasonable in order to obtain intense Raman peaks, since Raman intensities are inversely proportional to the fourth power of the wavelength [59]:

$$I_{max} \propto 1/\lambda^4 \tag{3.1.}$$

Although both Raman and IR are spectroscopic methods that provide information about the vibrational frequencies, Raman is superior for several reasons. First, the spatial resolution obtained in Raman is at least 1 order of magnitude higher than in IR as the resolution is directly dependent on the wavelength of the light source used. Secondly, the unique features of the confocal Raman microscope technique give both lateral resolution and depth resolution. The confocal hole only allows the Raman backscattered light from a chosen sample volume to reach the spectrometer. This constraint lowers the total intensity of the collected light but at the same time also reduces unwanted features. Optimizing the size of the focal hole is therefore a trade-off between optimal spatial resolution, total intensity, and signal to noise ratio. [61]

In general, a molecular vibration is IR-active, Raman-active or both and therefore one technique supplements the other one. [35]

4. Experimental

In this thesis three main objectives were investigated:

1. influence of the degree of crosslinking on thermal stability of EVA
2. Acetic acid transmission rate of EVA and backsheets
3. Effect of external stresses (UV/T, DH) and module composition on formation of acetic acid (GC/MS) and EVA degradation (UV/Vis/NIR and Raman spectroscopy)

Therefore, minimodules consisting of two types of EVA and four types of backsheets were prepared.

4.1. Thermogravimetric analysis (TGA)

Thermal properties of EVA FC and EVA STR 15580 with different degree of crosslinking were investigated by thermogravimetric analysis using Mettler Toledo TGA/DSC 1 ST**A**R^{e}System. The measurements were evaluated with MettlerST**A**R^{e} Default DB V10.00 software. Dynamical measurements were conducted in nitrogen and oxygen atmosphere with gas flow of 30 ml/min. Mass of samples was from 7 to 10 mg.

Dynamical measurements were performed according to the next method:

1. Samples were held isothermally for 5 minutes at the temperature of 25°C
2. Heating from 25°C to 400°C
3. Heating from 400°C to 900°C to remove impurities in crucible

Gas flow was 30 ml/min with a heating rate of 10 K/min.

In Figure 4.1. the TGA curve with typical points is represented. The T_1 and T_2 values represent the temperatures at which degradation of each step starts, while $T_{1\ max}$ and $T_{2\ max}$ represented the temperatures of maximum degradation for each step. The Mass loss of material that occurs in each step of degradation is marked with Δm. Mass of residue which refers to mass of inorganic part of material is marked with m_f.

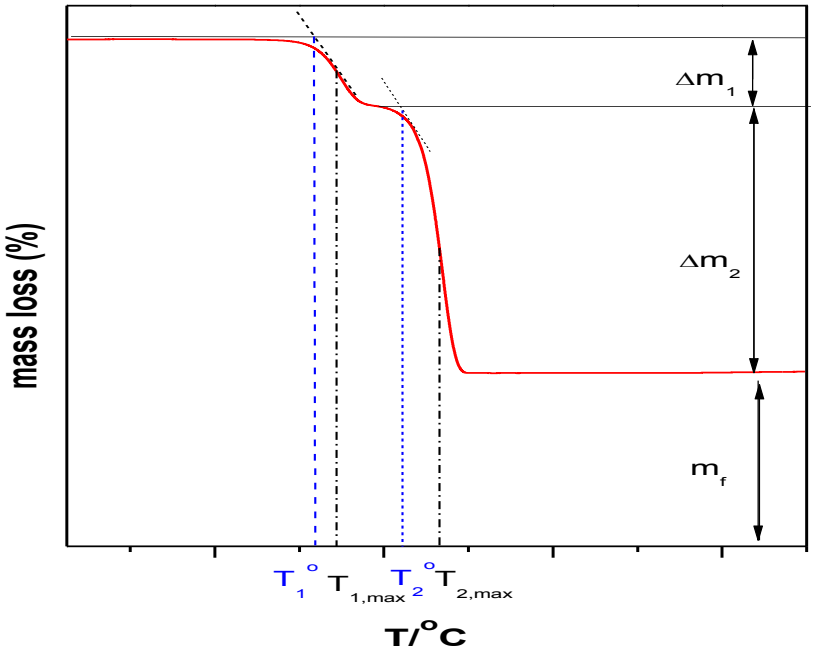

Figure 4.1. Interpretation of TGA curve

4.2. Gravimetric method – Acetic acid transmission rate of encapsulants and backsheets

Materials used in experiments are listed in Table 5.1. The transmission rate of acetic acid was measured by gravimetric method. In vials (dimension 45x14.75 mm) cca 1000 µL of acetic acid (Sigma-Aldrich 99%) was placed. The cap of each vial (d = 12 mm) contained a septum which was disassembled in order to make a hole (d = 9 mm) within a septum. The circular samples (d = 12 mm) of encapsulants as well as backsheets were cut out, placed within a cap and sealed with septum. The vials containing acetic acid were placed at room temperature (25°C) and in ovens (Heraeus, Germany) at different temperatures: 65, 85°C. Vials were exposed up to 1000h. Vials containing acetic acid were taken out from oven in order to measure change in mass. According to mass loss of acetic acid, Arrhenius plot "mass vs. time" was constructed. Slope of plot g/day was used in calculations of transmission rate according to equation 4.1.:

$$AATR = \frac{m}{(A * t)} \tag{4.1.}$$

where *AATR* (g/m^{2}day) is acetic acid transmission rate, *m* (g) is mass of permeating substance, *A*(m^2) is surface area of material through which permeation is obtained, while *t*

(day) is time in which permeation is monitored. Arrhenius plot "AATR vs. 1/T" was created and slope of that plot was used for calculation of activation energy of permeation of acetic acid according to Arrhenius law for different materials.

Table 4.1. Materials used in gravimetric method

	Material	Composition	Thickness/mm
Encapsulants	EVA FC S10	EVA	0.422
	EVA STR S10	EVA	0.411
Common backsheets	TPT	PVF/PET/PVF	0.332
	KPK	PVDF/PET/PVDF	0.329
	PPE/Alu	PE/PET/Alu/PET	0.388
	PPE	PE/PET/PET	0.365
	AAA	PA/PA/PA	0.370
	APA	PA/PET/PA	0.361
	THV	THV/PET/EVA	0.44
	EXP	PE/PE/PE	0.485
	ECTFE	ECTFE/PET/ECTFE	0.263
Fluoropolymers monolayers	Nowoflon THV	THV	0.2
	Nowoflon FEP	FEP	0.257
	Nowoflon ETFE	ETFE	0.246
	Nowoflon PVDF	PVDF	0.298
	Halar ECTFE	ECTFE	0.124
	PVF	PVF	0.144
PET monolayers	PET 4	PET	0.44
	RNK 50	PET	0.106
	LHA 50	PET	0.263
	RUVK 19	PET	0.304

4.3. Effect of external stresses (UV/T, DH) and module composition on formation of acetic acid and EVA degradation

4.3.1. Preparation of minimodules

Preparation of minimodules consisting of glass/EVA/backsheets was conducted in KIOTO PV. Materials used in preparation of minimodules are listed in Table 4.2.

Table 4.2. Overview of materials used in preparation of minimodules

	Name	Material	Company
Encapsulants	EVA STR 15580	Ethylene-vinyl-acetate	Specialized Technology Resources, Inc.
	EVA SKY	Ethylene-vinyl-acetate	Bridgestone
Backsheets	AAA	PA/PA/PA	Isovoltaic GmbH
	APA	PA/PET/PA	Dunmore Corp.
	PPE/Alu	PE/PET/Alu/PET	PPE Flexible AB
	PPE	PE/PET/PET	PPE Flexible AB

Laminated samples were cured in a vacuum lamination press. Encapsulants and backsheets were laminated together with glass. Dimension of samples was approximately 10x10 cm and they were later cut off in circular shape (d = 7.5 cm). Two layers of encapsulants and one layer of backsheet were used. No sealant was applied on the edges of the laminate. The lamination process took 9 minutes and 20 seconds, under the pressure of 850 mbar and temperature of 150°C. The thickness of laminates was around 436-477 μm. Each composition of minimodules was double prepared for two different ageing exposures.

The backsheets alone were cut off in squares (5x5 cm) and were cured in Heraeus Vakutrockensschrank VT laboratory oven at 150°C and 850 mbar for 10 minutes. They were also aged in the same way as minimodules in order to examine inner side of backsheets that is unreachable within PV module. Obtained information were used to track origin of yellowing in EVA.

Capsules for minimodules (see Figure 4.2.) were produced at WPK Kunststofftechnik. They were made out of stainless steel with diameter around 8 cm. Special precision O-ring and grease were used to accomplish sufficient sealing. Septum was placed at the bottom of the capsules. It was used for taking out gas from capsule via gas proof syringe (50μl, SGE Analytical Science, Australia) without opening a capsule. The taken gas was afterwards examined via GC/MS method in order to detect acetic acid that permeated to the backside of minimodules.

Figure 4.2. Capsule with minimodule from front- and backside

4.3.2. Artificial ageing of samples

4.3.2.1. Photo-oxidative ageing process

Capsules with minimodules, as well as backsheets alone, were exposed to artificial ageing. In order to examine photo-oxidative ageing processes, samples were aged in Suntester CPS+ (Atlas Materials Testing Technology GmbH, Germany) according to method ISO 4892-2 with an irradiance of 765 W/m^2 and with the black standard temperature within machine of 90°C throughout the exposure. It is necessary to point out that since this was first time to use this kind of capsule for minimodules and due to testing this method in short time, parameters for photo-oxidative ageing were adjusted. Samples were exposed up to 150h.

4.3.2.2. Thermo-oxidative ageing process

In order to support thermo-oxidative ageing processes, samples were exposed to damp heat ageing (DH). Samples were placed in Climate Chamber WKL^{64} (Weiss Umwelttechnik GmbH, Austria). Standard method according to IEC 61215 requires 85°C and 85% of relative humidity (RH). In this work, 90°C and 90% RH were applied for the same reason as with Suntester CPS+. Samples were also exposed up to 150h.

In both cases of aging, vapor on the backside of minimodules was sampled after 48h and 150h of exposure and examined via GC/MS. Also, minimodules were taken out in order to examine effect of acetic acid formation on degradation of PV modules via spectroscopic methods (UV/Vis/NIR and Raman spectroscopy).

4.4. Gas chromatography with mass spectrometry

Gas chromatography combined with mass spectrometry (GC/MS) measurements were conducted on instrument Shimadzu GC/MS-QP 2010 Plus equipped with AOC -20i (Autosampler). Column in instrument was Optima-5-Accent-0,25 µm (Fused Silica Capillary Column). Calibration of instrument was done with samples of pure ethanol, pure acetic acid

and acetic acid dissolved in ethanol in different concentrations. Injection volume for calibration was 1µL with split ratio 1:500. Injection volume of measurements was 50µL with split ratio 1:5. Therefore, it was necessary to do calculations in order to adjust different split ratios and to recalculate concentration of detected acetic acid from µL/µL into mol/µL.

4.5. Ultraviolet/Visible/Near-infrared (UV/Vis/NIR) spectroscopy

Analysis of optical properties of unaged and aged samples was obtained at Lambda 950 (Perkin Elmer, Germany) with an integrating sphere of Labsphere with spectralon coating and 150 mm diameter. Measuring range was between 250 and 2500 nm wavelength and the spectra was calculated according to AM 1.5 standard weighting from three independent measurements of each sample. PV modules were measured in reflection mode. For every experiment hemispheric measurements were performed. The spectrum was evaluated with the Spectrum 10 software.

4.6. Raman Spectroscopy

The Raman spectra of unaged and aged PV modules were measured with a confocal spectrometer named LabRAM HR 800 (Horiba JobinYvon GmbH, Germany). Circular samples (d = 7.5 cm) were irradiated with green laser (λ = 514 nm) in the Raman shift range of 650 - 4500 cm^{-1}. Holesize of 300 µm, 100 µm slit size and 600 g/mm (grooves/millimeter) grating were used. The 15 scans for one spectrum were performed and irradiation time was 5 seconds for every scan. The baseline correction and evaluation of the spectra were made with a LabSpec 5 Software. The 1439 cm^{-1} was chosen for normalization because it is found to be the least affected by the changes in the Raman shift range between 2000 and 650 cm^{-1}. Aged samples were measured after 48h and 150h of exposure.

5. Results and discussion

5.1. Thermogravimetric analysis

The influence of the degree of crosslinking on the thermal stability of EVA FC and EVA STR 15580 was investigated via thermogravimetric analysis (TGA) in inert (N_2) and oxidative (O_2) atmosphere. Dynamical measurements were conducted in order to examine influence of degree of crosslinking on temperature of 5% mass loss of material ($T_{5\%}$) which is usually taken as start of degradation, as well as temperatures of maximum thermal degradation (T_{max}). Since EVA usually shows two steps of degradation, T_{1max} and $T_{2\ max}$ are found in TGA curve of EVA. A typical TGA curve of EVA is shown in Figure 5.1.

In Figure 5.1. it can be seen that EVA shows a two steps of degradation. The first step of degradation occurs in a temperature range around 300-400˚C and is caused by elimination of acetic acid which leads to formation of an ethylene structure on the rest of the carbon chain. Hence, the second step of degradation i.e. the degradation of main chain occurs around 425 ˚C and is obtained by mechanism of chain cleavage. [30,48,64]

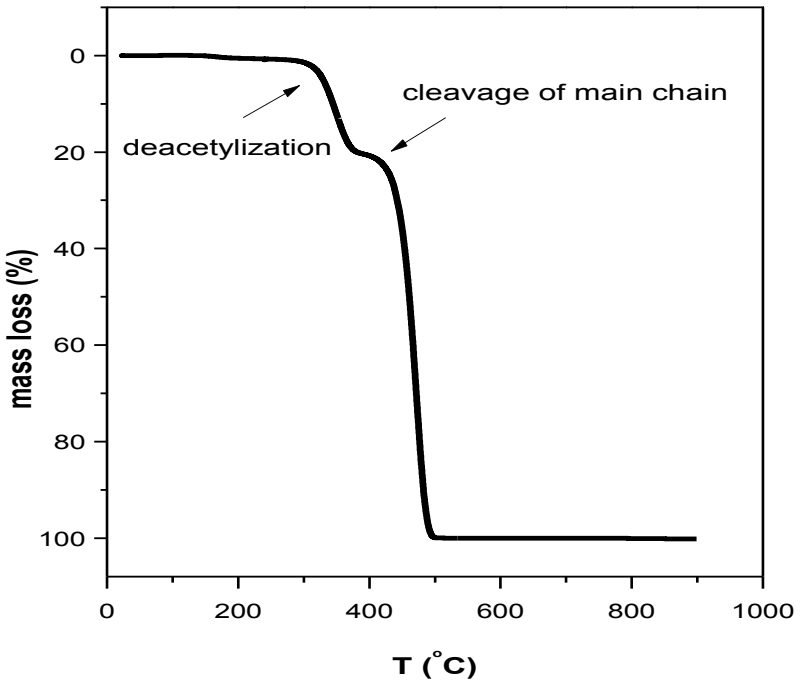

Figure 5.1. Typical TGA curve of EVA

Samples used in this work also showed two steps of degradation in dynamical measurements in inert and oxidative atmosphere (see Figure 5.2. and Table 5.1.). In Figure 5.2. can be seen that all samples, regardless to degree of crosslinking showed two steps of degradation in dynamical measurements. First step of degradation or deacetylation occurred around 350˚C in inert and around 340˚C in oxidative atmosphere. Second step of degradation i.e. cleavage of main chain occurred around 465˚C in both atmospheres. There is also an initial gain in weight (Figure 5.2. right) prior to deacetylation in the presence of oxygen which is due to a rapid initial oxidation of the polymer. [30] Also, it can be seen that samples in oxidative atmosphere showed higher mass loss in first step of degradation (Δm_1) which is probably due to incorporation of O_2 in structure of EVA that evaporated and resulted in higher mass loss.

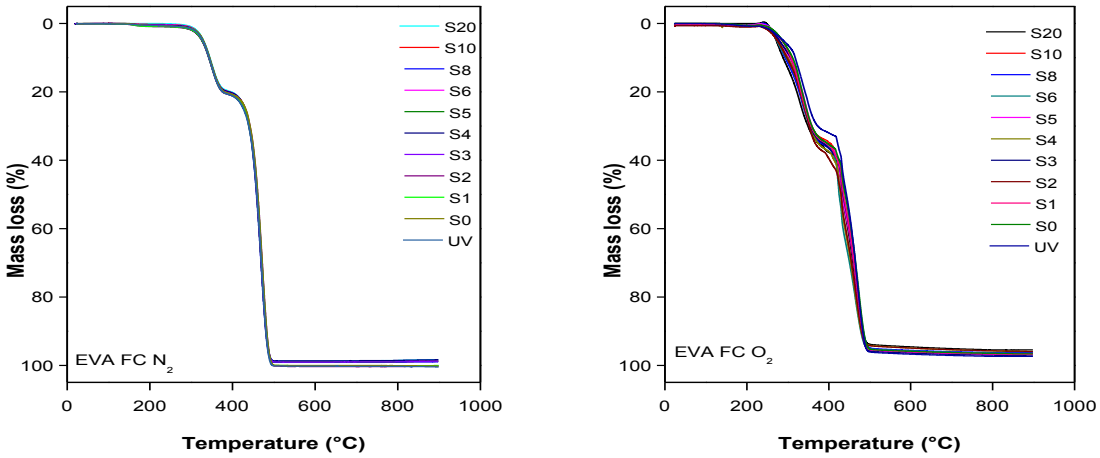

Figure 5.2. TGA curve for dynamical measurements of EVA FC in inert (left) and oxidative atmosphere (right)

According to results shown in Table 5.1. it can be seen that there are no significant changes in value of onset temperature $T_{5\%}$, as well as T_{1max} and T_{2max} regarding the degree of crosslinking. As expected, temperatures of $T_{5\%}$, T_{1max} and T_{2max} are slightly lower for oxidative than for inert atmosphere.

Table 5.1. Values of $T_{5\%}$, T_{1max} and T_{2max} for EVA FC in inert and oxidative atmosphere regarding to different degree of crosslinking

EVA FC / degree of crosslinking	$T_{5\%}$ (˚C)		T_{1max} (˚C)		T_{2max} (˚C)		Δm_1 (%)		Δm_2 (%)		m_f (%)	
	N_2	O_2	N_2	O_2	N_2	O_2	N_2	O_2	N_2	O_2	N_2	O_2
UV	329.06	287.95	349.26	348.43	472.3	466.5	20	33.54	80	64.26	0	2.2
S0	328.4	287.95	349.93	329.06	470.21	473.9	21	37.15	79	60.05	0	2.8
S1	329.04	287.02	348.57	329.76	472.31	473.96	21.6	36.2	78.4	60.7	0	3.1
S2	326.9	271.89	349.43	329.42	470.44	467.87	22	37.4	78	58.5	0	4.1
S3	325.9	278.89	349.13	337.42	468.43	466.19	21.5	40.3	77.3	57.3	1.2	2.4
S4	330.8	274.72	350	332.18	467.08	466.5	21.3	39.7	77	56.7	1.7	3.6
S5	326.32	281.44	348.89	339.59	465.71	473.38	23	37.9	75.8	59.2	1.2	2.9
S6	329.4	274.64	348.87	340.2	467.97	466.83	21	37.4	78.3	59.2	0.7	3.4
S8	327.83	274.96	345.49	332.46	469.69	467.11	20.7	38.4	79.3	58.2	0	3.4
S10	328.16	276.4	349.45	344.71	476.05	470.4	21.5	35.9	77.3	61	1.2	3.1
S20	329.47	270.88	349.5	328.55	469.4	462.56	22.5	40	76.3	56.1	1.2	3.9

Oxidative atmosphere showed the most influence on value of $T_{5\%}$ (Figure 5.3. left) which is probably due to aforementioned oxidation of material that caused faster degradation, while values of T_{1max} and T_{2max} showed no remarkable changes comparing to inert atmosphere (see Figure 5.3. right).

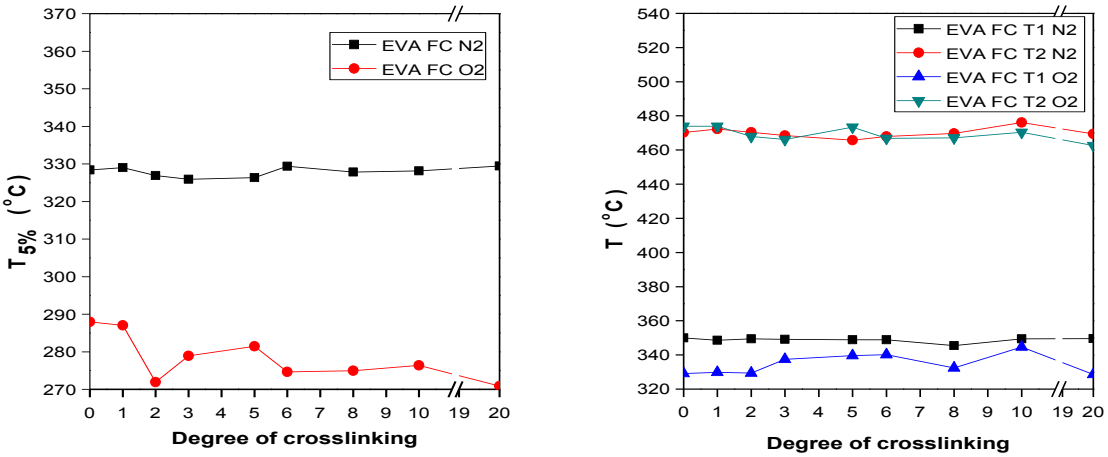

Figure 5.3. Influence of degree of crosslinking on value of $T_{5\%}$(left) and T_{1max} and T_{2max} (right) in inert and oxidative atmosphere

Another group of samples, EVA STR 15580 were also examined in the same conditions as EVA FC. Results are shown in Figure 5.4. and Table 5.2. Samples of EVA STR 15580 in dynamical measurements also showed two steps of degradation as well as EVA FC. Values of $T_{5\%}$, T_{1max} and T_{2max} are lower in oxidative atmosphere than in inert atmosphere (see Figure 5.5.). There is also an initial gain in weight like in EVA FC (Figure 5.4. right) observed. Difference in mass loss within first step of degradation (Δm_1) between inert and oxidative atmosphere is observed, which is a consequence of oxidation of the material and evaporation of oxygen. In Figure 5.4. (left) slight shift of the curve around 450˚C is observed. It is probably due to hydroperoxides used in production of EVA STR 15580.

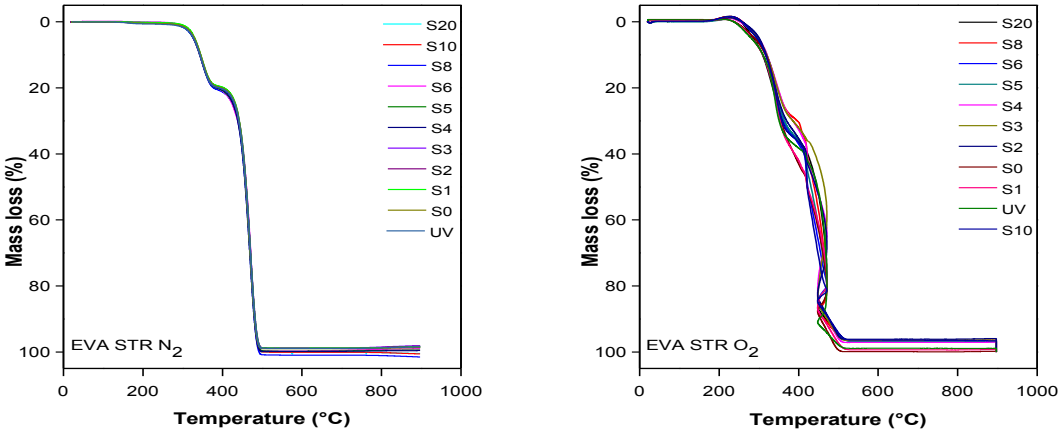

Figure 5.4. TGA curve for dynamical measurements of EVA STR 15580 in inert (left) and oxidative atmosphere (right)

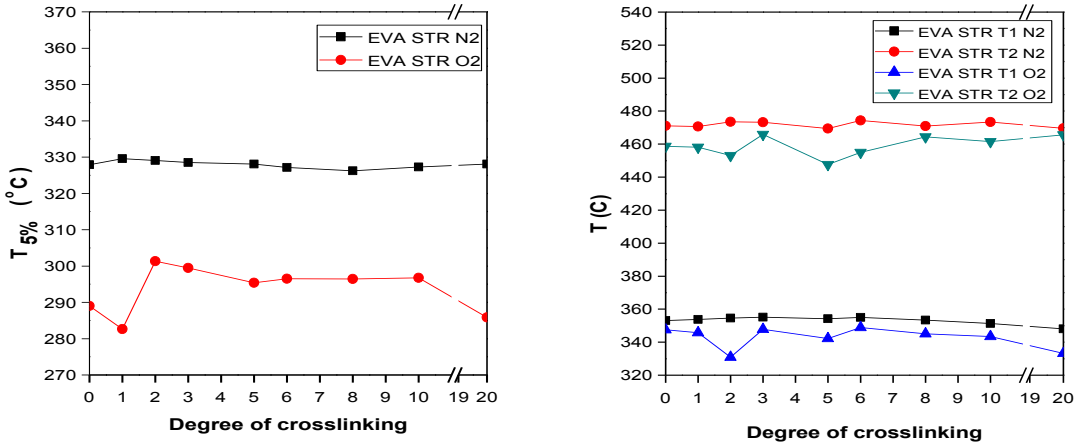

Figure 5.5. Influence of degree of crosslinking on value of $T_{5\%}$ (left) and T_{1max} and T_{2max} (right) in inert and oxidative atmosphere

Table 5.2. Values of $T_{5\%}$, T_{1max} and T_{2max} for EVA STR 15580 in inert and oxidative atmosphere regarding to different degree of crosslinking

EVA STR 15580 / degree of crosslinking	$T_{5\%}$		T_{1max}		T_{2max}		Δm_1 (%)		Δm_2 (%)		m_f (%)	
	N_2	O_2	N_2	N_2	O_2	N_2	N_2	O_2	N_2	O_2	N_2	O_2
UV	327.32	281.96	353.92	342.04	473.09	484.22	22	40.02	76.5	59.48	1.5	0.5
S0	327.9	289	353.13	347.51	471.03	458.61	22.2	45.5	76.3	54.5	1.5	0
S1	329.56	282.63	353.83	345.73	470.7	458.16	21.3	38.8	77.5	60.5	1.2	0.7
S2	329.07	301.34	354.61	330.92	473.5	453.13	21.8	37.8	76.5	58.6	1.7	3.6
S3	328.54	299.48	355.08	347.81	473.21	465.87	21.3	34.3	77	62.6	1.7	3.1
S4	328.55	299.56	354.01	349.06	471.42	449.83	21.5	34.7	78.5	62.3	0	3
S5	328.05	295.36	354.21	342.2	469.4	447.64	22.7	36.4	77.3	60.2	0	3.4
S6	327.18	296.48	354.99	348.94	474.37	454.94	21.7	36.6	77.4	60.3	0.9	3.4
S8	326.23	296.41	353.38	345.06	470.98	464.39	22.4	30.9	77.6	65.5	0	3.6
S10	327.25	296.74	351.3	343.4	473.38	461.53	21.5	31.8	78.5	64.8	0	3.4
S20	328.06	285.83	348.05	333.25	469.58	465.58	21.7	36.6	78.3	60.9	0	2.8

Comparing EVA FC and EVA STR 15580 (see Table 5.1. and 5.2.) it is evident that process of deacetylation (T_{1max}) occurs at slightly higher temperatures in EVA STR 15580 than in EVA FC in inert and oxidative atmosphere. This behavior can be due to different formulation of EVA FC and EVA STR 15580. Still, the difference between these values is not that significant to describe one of materials more or less thermally stable. According to results of thermogravimetric analysis it can be said that degree of crosslinking had no influence on thermal stability of EVA FC and EVA STR 15580 samples.

5.2. Gravimetric method – Acetic acid transmission rate of encapsulants and backsheets

In order to examine permeation properties of different materials a gravimetric method was used. Permeation of acetic acid through different types of materials was examined at different temperatures (25˚C, 65˚C, 85˚C) and the activation energy of permeation was calculated. Mass of vials containing acetic acid was monitored within 30 days. Curve "mass vs. time" was made and transmission rates (AATR) were calculated according to slope of the curve. Slope of the Arrhenius plot "AATR vs. 1/T" was used to calculate activation energy of permeation of acetic acid for all groups of materials (see Table 5.3.5.7.).

It should be pointed out that in Figures 5.6., 5.8., 5.10., 5.12. curves "mass lose vs. time" are presented but in calculations slope of the curves "mass vs. time" was used. In Figure 5.6. curve "mass loss vs. time" at 85˚C is shown and it can be seen that acetic permeated in only four days at 85˚C. Only a small amount of acetic acid permeated through septum which can be seen on the blue curve.

In Table 5.3. the calculated values of transmission rate of acetic acid (AATR) for EVA are listed. Since EVA is monolayer, thickness of material was included in calculations. In Figure 5.7. Arrhenius plot "AATR vs. 1/T" is shown. Slope of that curve was used to calculate activation energy of permeation of acetic acid.

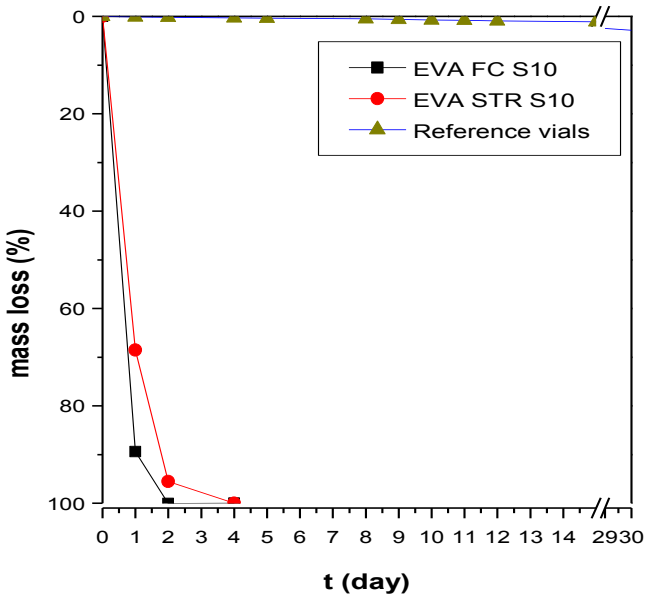

Figure 5.6. Mass loss of acetic acid through EVA at 85˚C

Table 5.3. Transmission rate of acetic acid for EVA

Material	Composition	Thickness (mm)	AATR (25˚C) (g*mm/m^2 day)	AATR (65˚C) (g*mm/m^2 day)	AATR (85˚C) (g*mm/m^2 day)
EVA FC S10	EVA	0.422	109.65	1262.07	3614.02
EVA STR 15580 S10	EVA	0.411	121.52	1103.0	3446.23

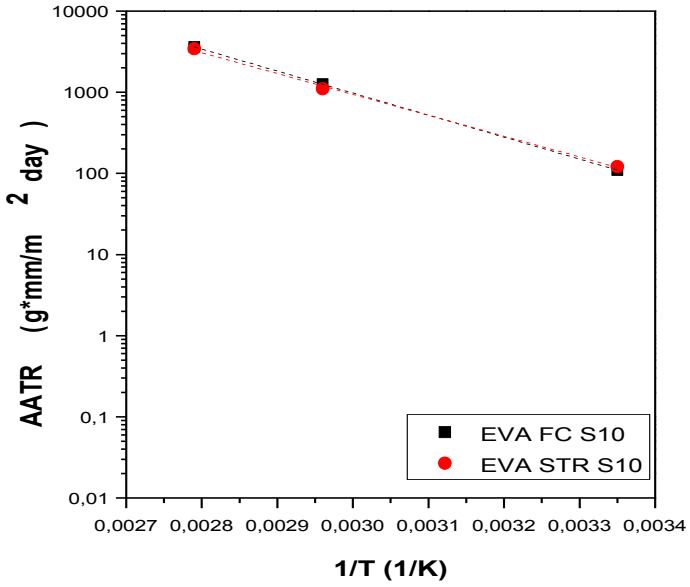

Figure 5.7. Arrhenius plot "AATR vs. 1/T" for encapsulant EVA

Table 5.4. Activation energy of permeation of acetic acid through EVA

Material	R	Ea (kJmol^{-1})
EVA FC S10	0.99	22.42
EVA STR 15580 S10	0.99	21.23

In Table 5.3. it can be seen that EVA FC and EVA STR 15580, as expected, showed very high transmission rates for acetic acid. EVA STR 15580 has slightly lower value of transmission rate although it has lower thickness. One reason for that can be a different formulation of EVA that affected the permeation of acetic acid or other molecules through the material. In Figure 5.7. it can be seen that permeation of acetic acid through EVA FC and

EVA STR 15580 showed linear behavior. Calculated Ea ($kJmol^{-1}$) values are similar (see Table 5.4.).

Figure 5.8. shows curves "mass loss vs. time" for common used backsheets. Table 5.5. lists calculated values for transmission rates of acetic acid for common used backsheets. All samples in the table are laminates of different materials. In case of multilayered samples, transmission rate refers to total transmission rate of sample and it depends on thickness and composition of each layer in structure. Figure 5.9a. - 5.9c. shows Arrhenius plot "AATR vs. 1/T" and calculated activation energy of permeation (see Table 5.6.).

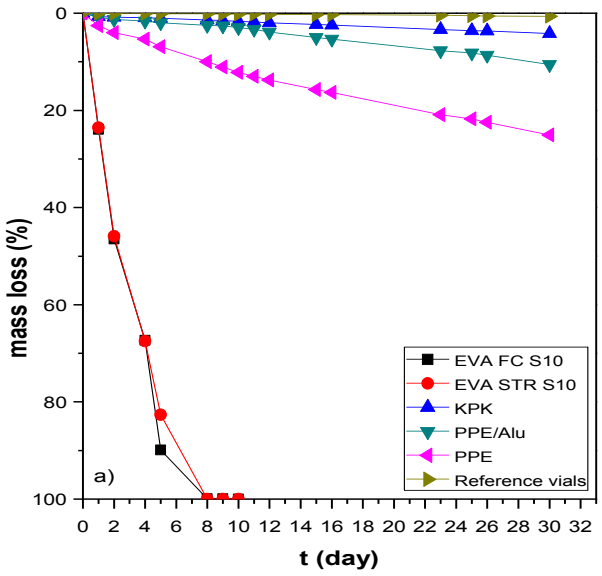

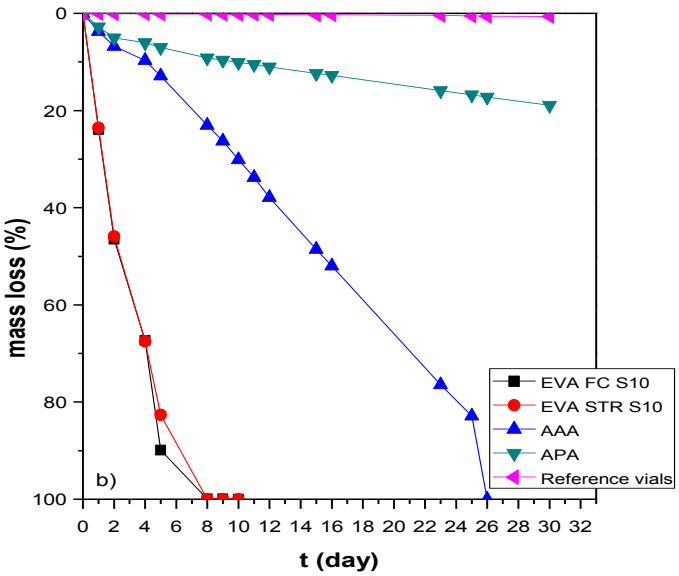

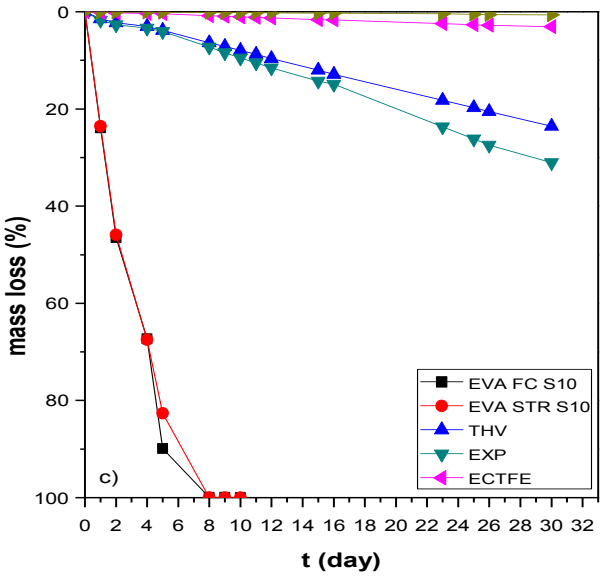

Figure 5.8. Arrhenius plot "mass loss vs. time" for common used backsheets

Table 5.5. Transmission rate of acetic acid for common used backsheets

Material	Composition	Thickness (mm)	AATR (25˚C) (g/m^2 day)	AATR (65˚C) (g/m^2 day)	AATR (85˚C) (g/m^2 day)
KPK	PVDF/PET/PVDF	0.329	5.01	23.74	68.69
PPE/Alu	PE/PET/Alu/PET	0.388	24.36	71.52	215.66
PPE	PE/PET/PET	0.365	76.71	149.80	183.28
AAA	PA/PA/PA	0.370	49.20	673.72	1330.30
APA	PA/PET/PA	0.361	/	92.43	107.36
THV	THV/PET/EVA	0.44	13.96	152.47	236.10
EXP	PE/PE/PE	0.485	30.49	209.38	306.83
ECTFE	ECTFE/PET/ECTFE	0.263	25.94	19.65	43.54

At room temperature laminate PPE showed the highest transmission rate of acetic acid (76.71 g/m^{2}day), while laminate KPK showed the lowest transmission rate (5.01 g/m^{2}day). Since during aging in climate chamber and UV chamber temperature of 85˚C was applied, transmission rates at 85˚C will be discussed. It can be seen (see Table 5.5.) that sample AAA showed the highest transmission rate of acetic acid among all other samples in the table. Reason for that behavior is composition of AAA, i.e. it is one of two samples that does not contain a PET as middle layer, which is known as good barrier layer. The other sample without PET as middle layer is EXP which also showed high transmission rates but still lower

values than AAA. Reasons for that behavior maybe the higher thickness of the EXP laminate or the degree of crystallinity of PE layer.

It can be seen that the laminate THV, even though containing a fluoropolymer and PET layer, showed high transmission rate of acetic acid. The reason for that is lower thickness of PET layer which is only 80 μm that must have affected permeation of acetic acid. Also, THV layer as outer layer is highly amorphous and therefore provides easier diffusion and permeation of acetic acid molecules.

Samples consisting of fluoropolymers as outer and inner layer and PET as middle layer (KPK and ECTFE), although being thinner than other samples, showed the lowest transmission rates. This is not surprising since fluoropolymers are known for its high degree of crystallinity and PET for its good barrier properties. Strong interactions between flouro atoms are influencing mobility of polymer chains which leads to lower permeation of permeating substance, respectively. Structure of PET includes aromatic rings that are known for decreasing chain flexibility and therefore reduction of penetrant diffusion. [41] Moreover, PET is a semi-crystalline polymer which is also a reason for reduced permeation. Lowest transmission rate is observed in laminate ECTFE/PET/ECTFE which is due to structure of ECTFE and off course of the PET layer. ECTFE is copolymer of PE and PCTFE. ECTFE is a partially crystalline polymer (λ_c= 50-55%) [65] and has very low transmission rate (Table 5.8.). Also, it contains chlorine atoms that form bonds with hydrogen atoms stronger than bonds between H and F atoms which affect polarity and permeability. Finally, when combined with PET layer, it has a very low transmission rate.

It may be strange that sample PPE (0.365 mm) which at room temperature and at 65˚C showed higher transmission rate than PPE/Alu (0.388 mm), at 85˚C showed lower transmission rate. This behavior could be the consequence of interactions between acetic acid and aluminum layer at elevated temperatures.

In Figure 5.9a. - 5.9b. it can be seen that common used backsheets have lower transmission rates of acetic acid compared to EVA. The lowest activation energies of permeation of acetic acid were calculated for samples APA and PPE, while the highest was for sample AAA.

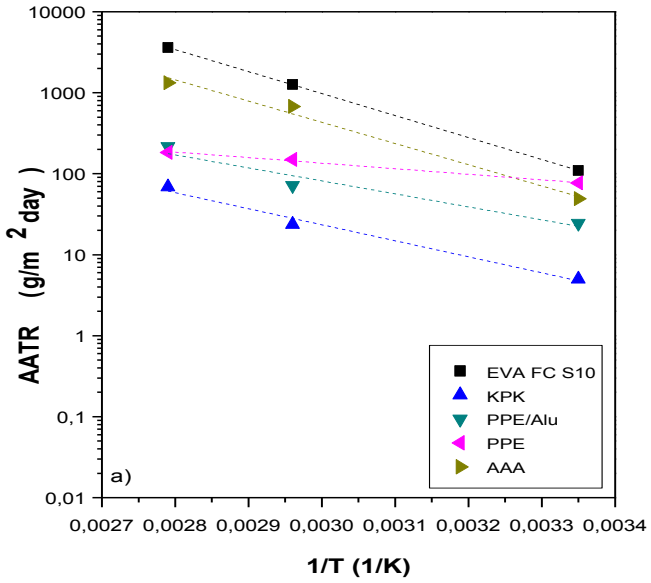

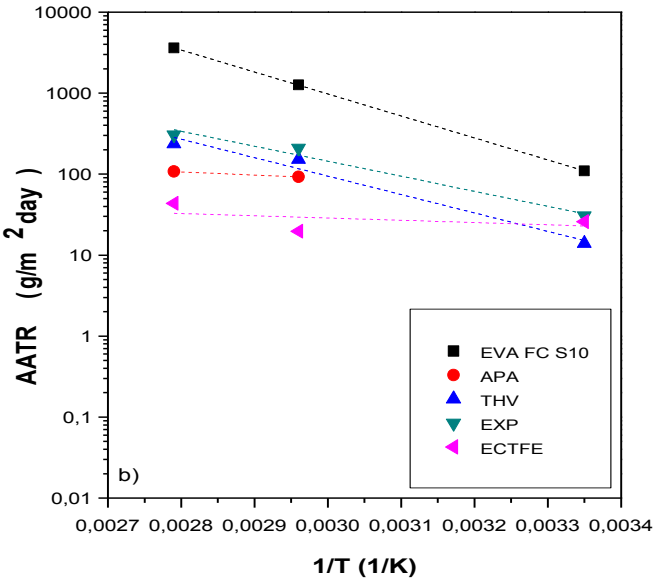

Figure 5.9. Arrhenius plot "AATR vs. 1/T" for common used backsheets

Table 5.6. Activation energy of permeation of acetic acid through common used backsheets

Material	R	Ea ($kJmol^{-1)}$
KPK	0.97	16.33
PPE/Alu	0.89	13.24
PPE	0.99	5.68
AAA	0.98	21.67
APA	1.00	3.27
THV	0.96	18.83
EXP	0.96	15.33

Table 5.7. lists transmission rates and activation energies of permeation of water vapour, oxygen and acetic acid. Those are the results of measurements obtained within work of [11]. It is important to point out that method of measuring used in this thesis is not the same as used in work of dr. Marlene Knausz and therefore values of activation energies and transmission rates given in Table 5.7. are used just to show the relation between results. It can be seen that WVTR values are lower than AATR values for all samples. Regarding to activation energies, it is evident that the lowest activation energy is required for transmission of oxygen, which can also be correlated with molecular weight of oxygen (32.00 g/mol) that is lower than molecular weight of acetic acid (60.05 g/mol).

Table 5.7. Values of WVTR, OTR and AATR for standard used backsheets at 85˚C

Material	WVTR ($g\ /m^2day$)	$Ea_{WV85^{\circ}C}$ ($kJmol^{-1}$)	AATR ($g\ /m^2day$)	$Ea_{AA85^{\circ}C}$ ($kJmol^{-1}$)	OTR ($cm^3*m^2\ day^{-1}\ bar^{-1}$)	$Ea_{O285^{\circ}C}$ ($kJmol^{-1}$)
KPK	7.86	37.2	68.69	16.33	99,5	9.5
PPE	10.63	35.3	183.28	5.68	89,3	4.3
AAA	18.63	42.5	1330.30	21.67	2642	17.2

Table 5.8. represents the calculated transmission rate values of acetic acid for several fluoropolymer monolayers. Since those are monolayers, the thickness of materials was

included in calculations. In Figure 5.10. Arrhenius plot "AATR vs. 1/T" is shown and calculated activation energies of permeation of acetic acid are listed (see Table 5.9.).

It can be seen in Table 5.8. that monolayer THV, although not being the thinnest material, showed the highest transmission rate of acetic acid among all fluoropolymer monolayers at all temperatures. It is not surprising since THV used in these experiments is highly amorphous with melting peak at around 162˚C and enthalpy at 10 J/g. Nevertheless, THV has glass transition temperature (Tg) around 34˚C and exposure to temperatures applied in experiments may affect mobility of polymer chains and therefore permeability. [15] On the other hand, monolayer ECTFE showed the lowest value of transmission rate at all temperatures. Reason for that behavior is in the structure of ECTFE, i.e. its crystallinity around 50-55% [65] and chlorine atoms that form strong bonds with hydrogen atoms which affects polarity and permeability. Also, it should be considered that the glass transition temperature (Tg) of ECTFE is around 85˚C. [65] Since below glass transition mobility of polymer chains is reduced, therefore lower permeation rates were observed at temperatures lower than 85˚C. Sample PVF is the second material after THV considering the transmission rate of acetic acid. PVF shows enthalpy value around 39 J/g which is higher than enthalpy of THV which is 10 J/g which had influence on permeation of acetic acid. Monolayer FEP has branched structure which resulted in melting enthalpy of 14 J/g and degree of crystallinity of about 16%. [15] Comparing transmission rates for FEP at 25˚C, 65˚C and 85˚C it can be seen that at 85˚C transmission rate is just slightly higher than at 65˚C. This behavior may be due to glass transition temperature (Tg = 76˚C) [15] that is in range of temperatures used in experiment, which could affect permeability of acetic acid molecules. Monolayer ETFE also showed lower transmission rates of acetic acid which is consequence of higher degree of crystallinity (in comparison with samples in Table 5.4.) that ranges from 28 to 40%. [15]

Table 5.8. Transmission rate of acetic acid for fluoropolymers used as layers in backsheets

Material	Composition	Thickness (mm)	AATR (25˚C) (g*mm/m^2 day)	AATR (65˚C) (g*mm/m^2 day)	AATR (85˚C) (g*mm/m^2 day)
Nowoflon THV	THV	0.2	11.13	355.06	926.73
Nowoflon FEP	FEP	0.257	0.03	39.43	41.85
Nowoflon ETFE	ETFE	0.246	5.68	6.81	21.04
Nowoflon PVDF	PVDF	0.298	1.23	40.38	69.61

Halar ECTFE	ECTFE	0.124	1.16	7.95	17.68
IsovoltaicPVF	PVF	0.144	3.53	70.08	216.46

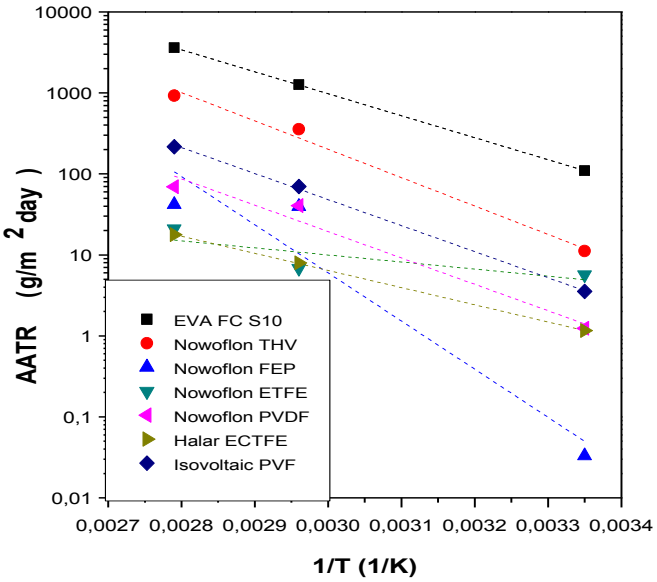

Figure 5.10. Arrhenius plot "AATR vs. 1/T" for fluoropolymer monolayers

Table 5.9. Activation energy of permeation of acetic acid through fluoropolymer monolayers

Material	R	Ea (kJ mol^{-1})
N. THV	0.99	28.98
N.FEP	0.84	49.32
N.ETFE	0.3	7.16
N.PVDF	0.95	26.98
Halar ECTFE	1	17.52
Isovolatic PVF	0.99	26.59

In Table 5.10. calculated values of transmission rates of PET based materials are listed. Thickness of monolayers was included in calculations. In Figure 5.11. Arrhenius plot "AATR vs. 1/T" for PET monolayers and calculated Ea values are represented (see Table 5.11.).

In Table 5.10. it can be seen that all samples have similar values of transmission rate of acetic acid at 85˚C. Sample RNK 50 (0.106 mm) showed the highest transmission rate, while PET 4 (0.44 mm) showed the lowest transmission rate, which is in accordance with thickness of

layers. As already stated PET is a semi crystalline polymer and a good barrier layer and therefore has a low value of transmission rate of acetic acid, especially at room temperatures.

Table 5.10. Transmission rate of acetic acid for PET used as layers in backsheets

Material	Composition	Thickness (mm)	AATR (25˚C) (g*mm/m^2 day)	AATR (65˚C) (g*mm/m^2 day)	AATR (85˚C) (g*mm/m^2 day)
PET 4	PET	0.44	/	10.78	5.83
RNK 50	PET	0.106	0.47	0.93	14.78
LHA 50	PET	0.263	0.88	3.15	14.15
RUVK 19	PET	0.304	0.25	3.22	13.82

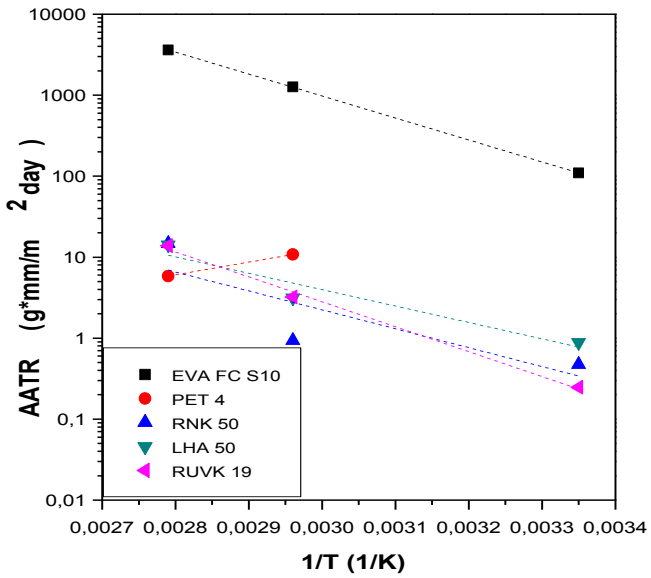

Figure 5.11. Arrhenius plot "AATR vs. reverse temperature" for PET monolayers

Table 5.11. Activation energy of permeation of acetic acid through PET monolayers

Material	R	Ea (kJ mol^{-1})
PET 4	/	/
RNK 50	0.42	19.17
LHA 50	0.85	16.69
RUVK 19	0.99	25.42

According to results shown in this chapter it can be seen how thickness, composition, and degree of crystallinity of materials influenced permeability of acetic acid through materials used in solar applications. EVA as encapsulation material showed the highest transmission rate of acetic acid. On the other hand, laminates containing PET as middle layer, as well as PET monolayers, showed lower transmission rates of acetic acid than samples without PET layer. Laminates containing fluoropolymers as outer/inner layer showed lower transmission rates (except laminate THV/PET/EVA) in comparison with laminates without fluropolymer layers. Regarding to transmission rates of acetic acid for fluoropolymer monolayers alone it is evident how morphology, i.e. degree of crystallinity and chemical composition affected permeability. The best transmission rates at 85˚C were observed in monolayers THV and PVF. The lowest transmission rate was observed in sample ECTFE due to additional chlorine atoms that caused stronger bonds with hydrogen and therefore reduced mobility of polymer chains.

5.3. Gas chromatography combined with mass spectrometry

Gas chromatography combined with mass spectrometry (GC/MS) measurements were conducted in order to investigate effect of external stresses (UV/T and DH) on formation of acetic acid within capsules containing different combinations of EVA (EVA STR 15580 and EVA Bridgestone) and backsheets (AAA, APA, PPE/Alu, PPE). Results of measurements, i.e. detected concentration of acetic acid formed within period of 48h of exposure under UV/T and DH conditions, are shown below in Figures 5.12. - 5.17. Since vapor containing acetic acid was sampled from backside of the minimodules, concentration detected via GC/MS measurements refers to concentration of acetic acid that permeated through backsheet.

In Figure 5.12. it can be seen that EVA STR (left) produced more acetic acid within the same period of exposure than EVA Bridgestone (right) which is probably due to higher content of vinyl acetate (VA%) in EVA STR that makes EVA STR more vulnerable. Transmission rate of acetic acid for EVA STR at 85 ˚C is 3446.2 (g*mm/m^2day) which is reason that 5.6 x 10^{-9} mol$\mu L^{-1}$of acetic acid easily permeated through EVA and was found on the backside of minimodule consisting only of glass and double layer of EVA. It is evident that minimodules combined with both types of EVA, APA/EVA and PPE Alu/EVA, showed higher concentration of permeated acetic acid in comparison with AAA/EVA and PPE/EVA under UV/T exposure. Since results obtained by gravimetric method showed that AAA has the highest transmission rate among backsheets used in minimodules, it may seem contradictory that AAA/EVA showed the lowest concentration of permeated acetic acid. But at this point, it

is necessary to emphasize that acetic acid acts as autocatalyst when formed in EVA, enhancing further production of acetic acid. AAA has transmission rate of 1330.30 (g/m^2day) at 85˚C, which is much higher than APA that has 107.36 (g/m^2day) (see Table 5.5.). Still, much less acetic acid was detected via GC/MS measurements in AAA/EVA than in APA/EVA. This could indicate that AAA in combination with EVA is less permeable to acetic acid. But, referring to acetic acid as an autocatalyst, explanation of this observation could be that AAA is more breathable and therefore acetic acid can easily permeate through AAA. On the other hand, APA has much lower transmission rate at 85 ˚C which causes retention of acetic acid on interface between EVA and backsheet. Retained acetic acid causes further degradation of EVA, i.e. production of acetic acid. Since APA has activation energy of permeation of acetic acid 3.3 $kJmol^{-1}$ it does not require much energy to „push“ formed acetic acid through interface to the back side of minimodule. Therefore, it is possible to detect acetic acid after 48h of exposure. For that reason, there is much more acetic acid detected on the backside of APA/EVA than in AAA/EVA.

The similar behavior was observed between samples PPE Alu/EVA and PPE/EVA. In Figure 5.12. (left) it can be seen that more acetic acid is detected in PPE Alu/EVA than in PPE/EVA (right). PPE Alu has transmission rate at 85 ˚C of 215.66 (g/m^2day) which is slightly higher than PPE which has transmission rate of 183.28 (g/m^2day). Although PPE Alu has higher transmission rate than PPE, measurements showed higher degradation of PPE Alu than PPE (see Chapter 5.4. and 5.5.). Reason for that could be the retention of acetic acid due to aluminum layer which causes additional production of acetic acid and higher degradation of EVA, i.e. aluminum layer acts as a barrier layer. Also, the reason for higher degradation could be the corrosion of aluminum layer at elevated temperatures due to acetic acid which enhanced degradation of EVA.

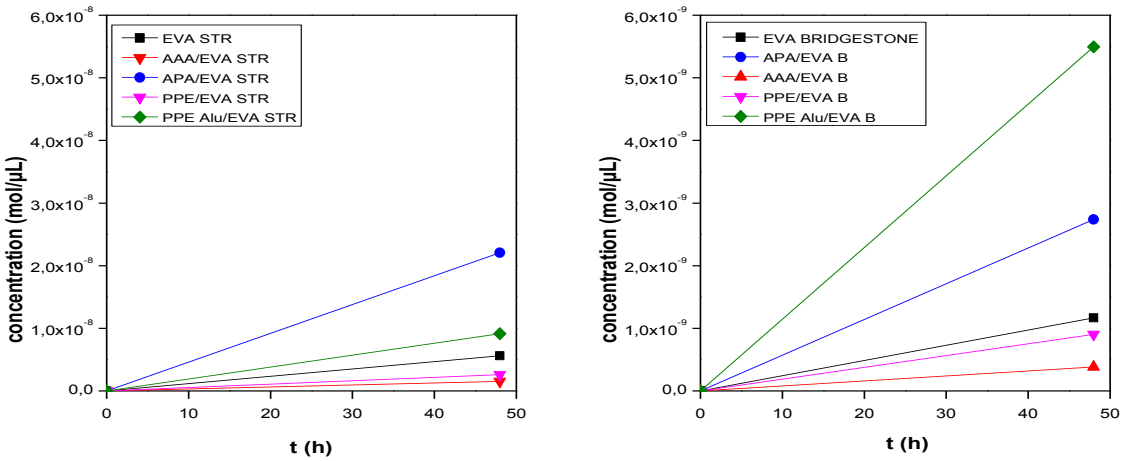

Figure 5.12. Concentration of acetic acid formed within 48 h of exposure to UV/T in EVA STR (left) and EVA Bridgestone (right)

Figure 5.13. shows the concentration of the formed acetic acid under DH within 48h of exposure in EVA STR and EVA Bridgestone. It is important to point out that undetected concentration of acetic acid at the backside of the APA/EVA STR is the consequence of mistake during measurement procedure. It can be seen that EVA STR under DH conditions produced less acetic acid ($1.6*10^{-9}$ molµL^{-1}) in comparison with EVA STR under UV/T conditions which leads to assumption that UV radiation i.e. photodegradation has more influence on degradation of EVA than damp heat in the same period of exposure (also see Figure 5.14.). Since there is no value for concentration of permeated acetic acid in APA/EVA STR, only the relation between PPE Alu- and PPE/EVA STR will be considered. Reason why PPE Alu/EVA STR showed higher concentration of acetic acid is the same as in case of UV/T exposure – retention of acetic acid at interface between EVA and backsheet.

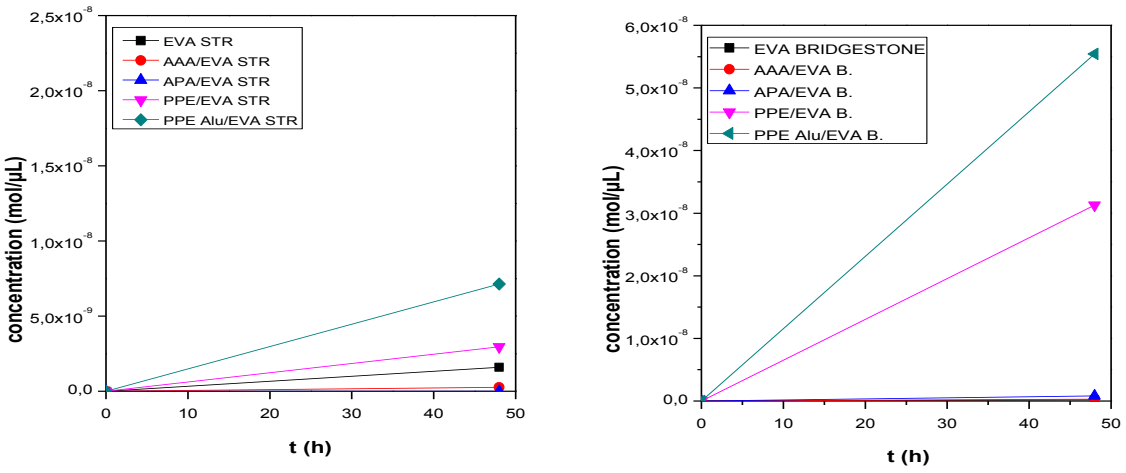

Figure 5.13. Concentration of acetic acid formed within 48 h of exposure under DH in EVA STR (left) and EVA Bridgestone (right)

Figure 5.14. shows a comparison of concentrations of formed and permeated acetic acid under UV/T and DH exposure. In Figure 5.14a. it can be seen that, in general, more acetic acid was produced in EVA STR than in EVA BRIDGESTONE. Also, UV/T exposure revealed in higher concentration of formed acetic acid than damp heat in both, EVA STR and EVA BRIDGESTONE. It can be said that UV/T exposure had more effect on formation of acetic acid, i.e. degradation of minimodules consisting only of EVA and glass. Figure 5.14b. and Figure 5.14c. show concentrations of formed and permeated acetic acid in AAA/EVA and APA/EVA minimodules. According to curves, it is evident that more acetic acid was formed and permeated under UV/T exposure than DH exposure. But when comparing samples of PPE/EVA and PPE Alu/EVA (see Figure 5.14d. and Figure 5.14e.) different behavior is observed. PPE/EVA BRIDGESTONE exposed to DH showed higher concentration of permeated acetic acid among other PPE/EVA samples. Still, PPE/EVA STR exposed to UV/T radiation showed slightly higher concentration of permeated acetic acid than PPE/EVA BRIDGESTONE in the same conditions. Only minimodule consisting of PPE Alu/EVA showed higher concentration under DH conditions for both types of EVA. So, according to results presented in Figure 5.14a. - Figure 5.14e. it can be said that minimodules combined with EVA STR and exposed to UV/T conditions showed higher concentration of formed and permeated acetic acid than samples exposed to DH (except PPE Alu/EVA STR). On the other hand, minimodules combined with EVA BRIDGESTONE showed slightly higher concentration of formed and permeated acetic acid under UV/T exposure (EVA BRIDGESTONE, AAA and APA/EVA BRIDGESTONE), but much higher concentration of acetic acid under DH conditions for PPE and PPE Alu/EVA BRIDGESTONE. Maybe a

reason for that behavior is the formulation of EVA STR and EVA BRIDGESTONE, i.e. different additives, or measurements procedure.

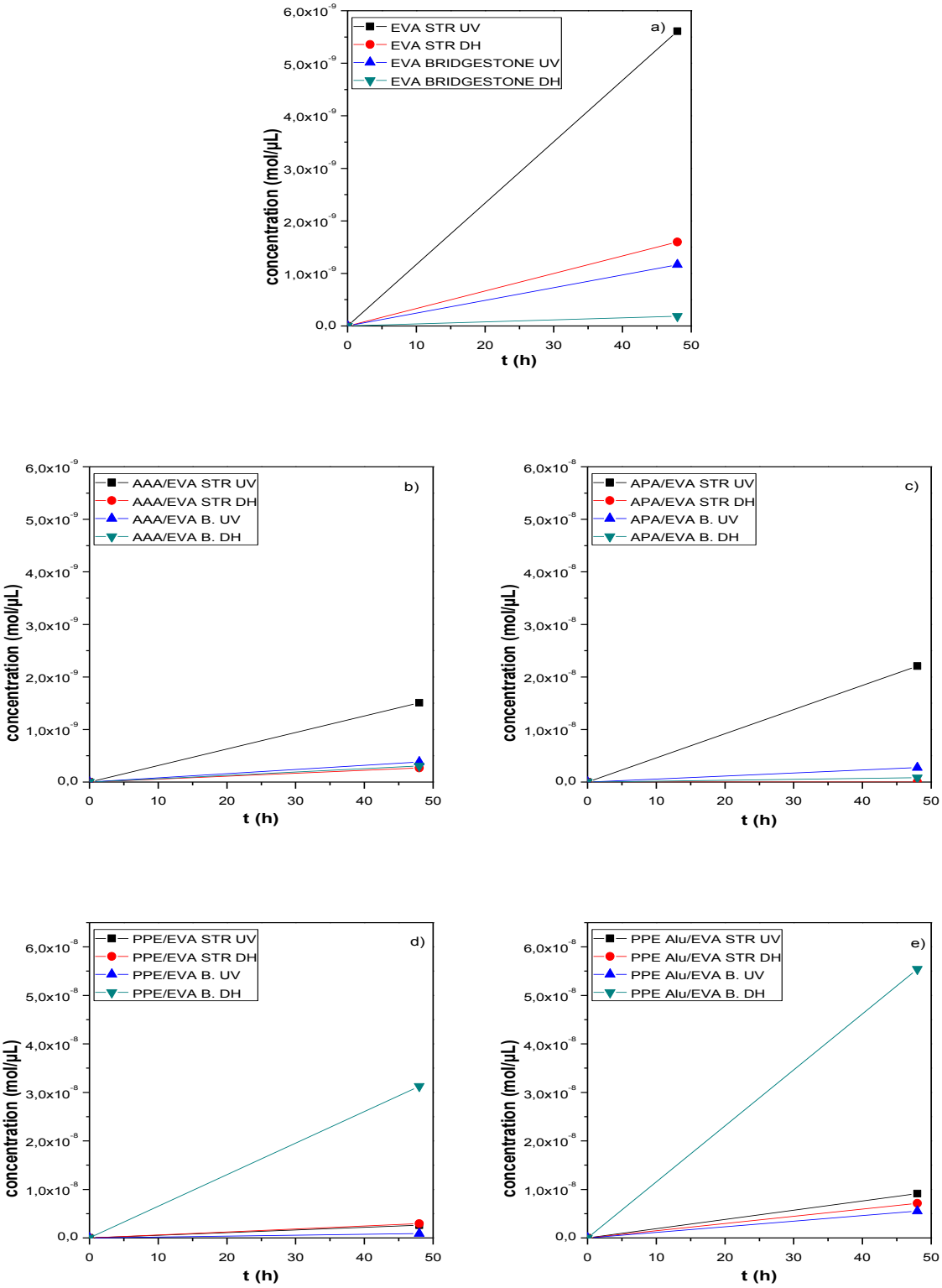

Figure 5.14. Influence of external stresses on formation and permeation of formed acetic acid

Since concentration of acetic acid is very low, the difference between values can be a consequence of measurement inaccuracies. Therefore, it is hard to state with only GC/MS measurements which exposure causes more degradation in minimodules. But according to results obtained by gravimetric method and GC/MS measurements, it can be said that AAA showed the highest transmission rate of acetic acid, i.e. it can be considered as most breathable backsheet among backsheets used in this work.

5.4. UV/Vis/NIR spectroscopy

Minimodules were examined via UV/Vis/NIR spectroscopy in order to investigate the origin of yellowing of EVA. Since inner side of minimodules was impossible to measure, inner side of backsheets that were aged together with minimodules was measured. Minimodules were measured with the glass cover and backsheet layer in hemispherical reflectance mode. Therefore, it has to be considered in the evaluation of the measurements that a spectrum of minimodules is a combination of the transmittance of the glass cover and EVA layer and of the reflection of the backsheet layer. The backsheet reflected the light back through the EVA layer and glass cover. So, reflection of parts of the light may occur at every layer. Obtained spectra in hemispherical reflectance mode are represented in Figure 5.15a. - 5.15j.

The UV/Vis/NIR spectra were measured in the range from 250 to 2500 nm but only the visible range from 250 to 800 nm is shown because there were no significant changes observed in region from 800 to 2500 nm.

In Figure 5.15. the results of UV/Vis/NIR measurements of minimodules and backsheets are presented. In Figure 5.15a. and Figure 5.15b. the spectra of EVA minimodules are represented. It can be seen that there is no significant change in UV region (250-400 nm) after UV/T radiation which means that there is no degradation of UV absorbers i.e. stabilizers after 150 h of exposure to UV/T conditions (see Figure 5.15a. and Figure 5.15b. red curves). In minimodule EVA BRIDGESTONE a slight drop in hemispherical reflectance after DH exposure can be observed.

In Figure 5.15c. and Figure 5.15d. spectra of unaged and aged backsheet AAA, AAA/EVA STR and AAA/EVA BRIDGESTONE are represented. It can be seen that aged backsheets have higher hemispherical reflection than aged minimodules (laminates) of AAA/EVA, which is expected due to composition of minimodules. Backsheet AAA exposed to UV/T radiation and DH showed slight increase of reflection in range of 400-600 nm, i.e. around cut off. The cut off is the point between UV and the visible region where reflection/transmission of the sample drops to the values close to zero. [35]

On the other hand, minimodule of AAA/EVA STR under UV/T radiation showed no significant changes in comparison with unaged minimodule, while minimodule aged in DH conditions showed drop in reflection around cut off. Minimodule AAA/EVA BRIDGESTONE showed no significant changes in cut off region, but slight increase of reflection at wavelengths higher than cut off were observed.

In Figure 5.15e. and Figure 5.15f. UV/Vis/NIR spectra for APA backsheet, APA/EVA STR and APA/EVA BRIDGESTONE minimodules are represented. Comparing the spectra of aged backsheet APA under UV/T and DH conditions, no significant changes in spectra are observed. On the other hand, minimodules made of APA/EVA STR and APA/EVA BRIDGESTONE showed a different behavior. The drop of the reflection around the cut off region was observed in minimodules APA/EVA aged under UV/T radiation. Minimodule APA/EVA STR aged in DH conditions showed increase in reflection from 400 to 1500 nm, while minimodule APA/EVA BRIDGESTONE showed slight drop in reflection around cut off region and increase in reflection that started around 500nm. Minimodules PPE/EVA STR and PPE/EVA BRIDGESTONE (see Figure 5.15g. and Figure 5.15h.) showed drop of reflectance around cut off region in backsheet of PPE but also in minimodules after UV/T and DH exposure. The same behavior was observed in minimodules PPE Alu/ EVA (see Figure 5.15i. and Figure 5.15j.).

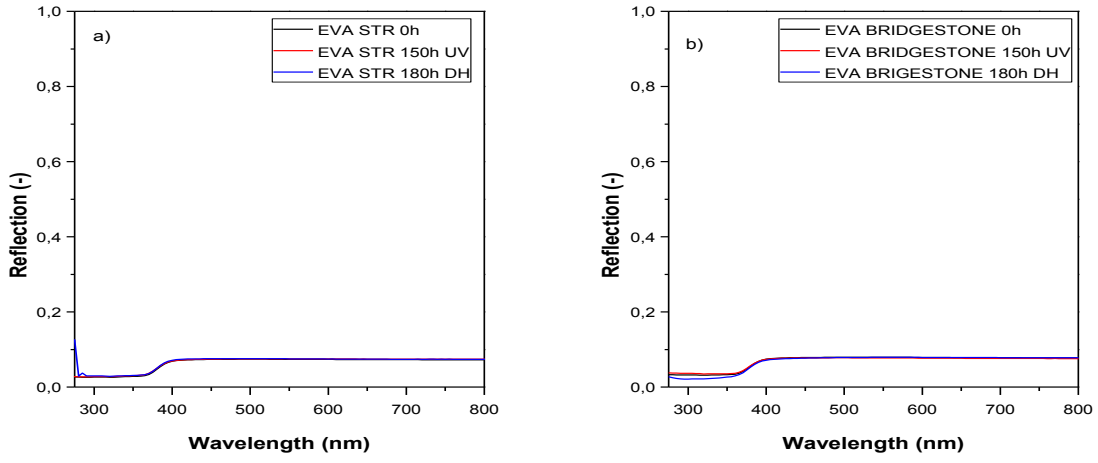

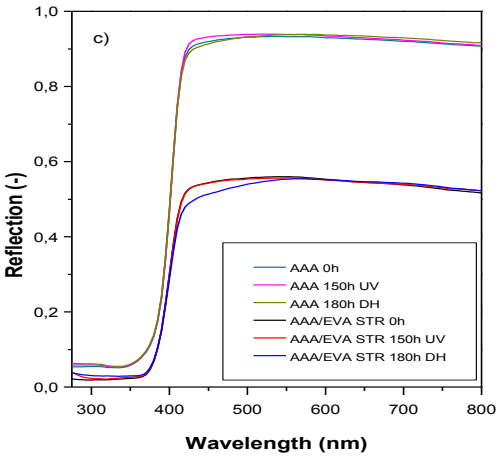
c)
Reflection (-)
Wavelength (nm)
AAA 0h
AAA 150h UV
AAA 180h DH
AAA/EVA STR 0h
AAA/EVA STR 150h UV
AAA/EVA STR 180h DH

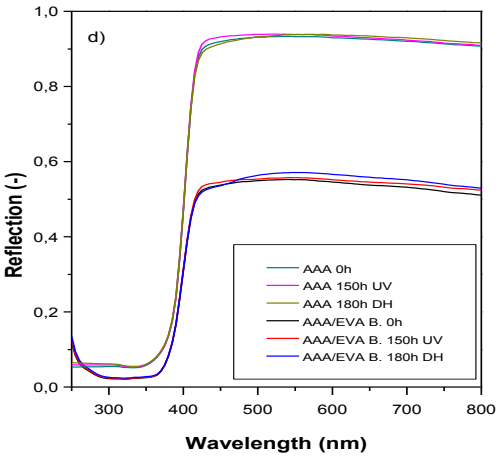
d)
Reflection (-)
Wavelength (nm)
AAA 0h
AAA 150h UV
AAA 180h DH
AAA/EVA B. 0h
AAA/EVA B. 150h UV
AAA/EVA B. 180h DH

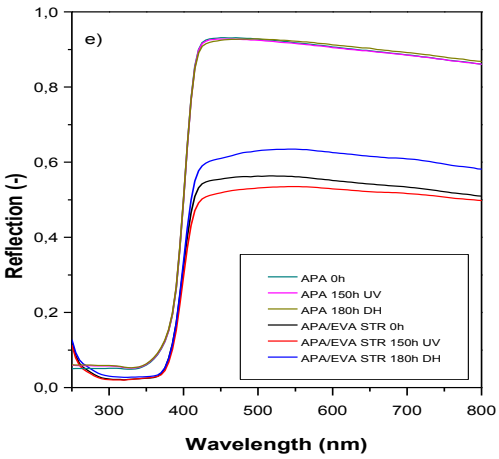
e)
Reflection (-)
Wavelength (nm)
APA 0h
APA 150h UV
APA 180h DH
APA/EVA STR 0h
APA/EVA STR 150h UV
APA/EVA STR 180h DH

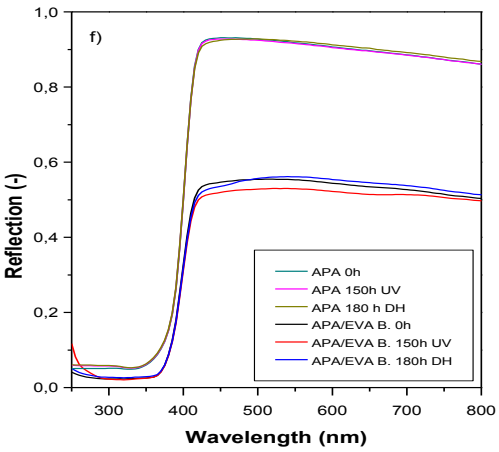
f)
Reflection (-)
Wavelength (nm)
APA 0h
APA 150h UV
APA 180 h DH
APA/EVA B. 0h
APA/EVA B. 150h UV
APA/EVA B. 180h DH

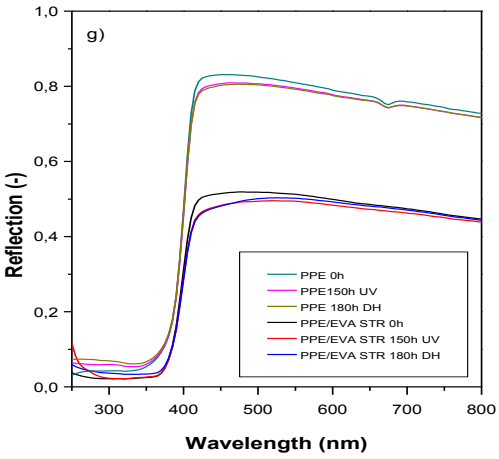
g)
Reflection (-)
Wavelength (nm)
PPE 0h
PPE150h UV
PPE 180h DH
PPE/EVA STR 0h
PPE/EVA STR 150h UV
PPE/EVA STR 180h DH

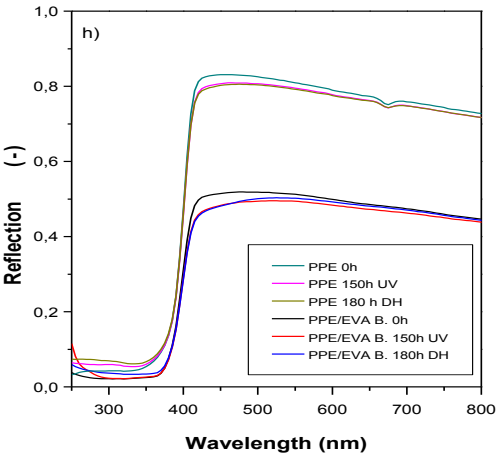
h)
Reflection (-)
Wavelength (nm)
PPE 0h
PPE 150h UV
PPE 180 h DH
PPE/EVA B. 0h
PPE/EVA B. 150h UV
PPE/EVA B. 180h DH

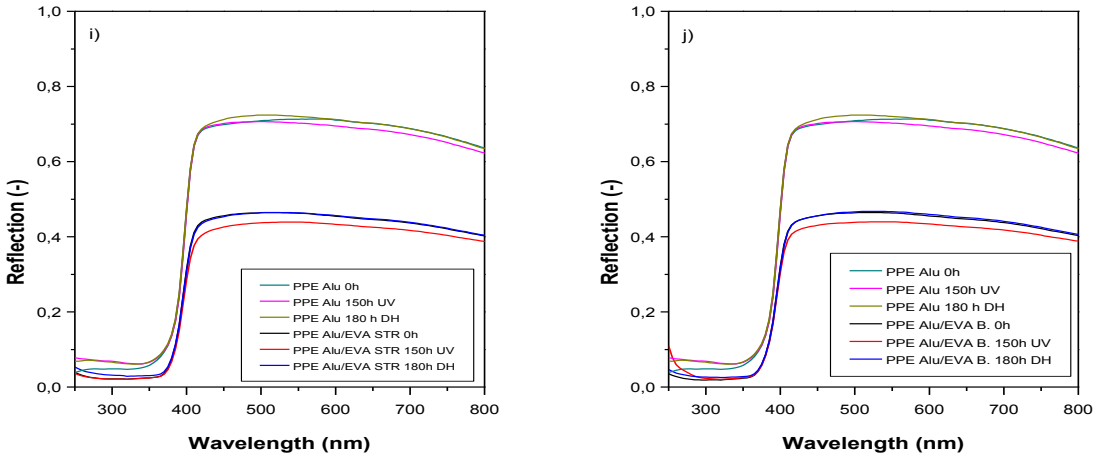

Figure 5.15. Spectra of unaged and aged minimodules and backsheets:a) EVA STR, b) EVA BRIDGESTONE, c) AAA/EVA STR; d) AAA/EVA BRIDGESTONE; e) APA/EVA STR; f) APA/EVA BRIDGESTONE; g) PPE/EVA STR; h) PPE/EVA BRIDGESTONE; i) PPE Alu/EVA STR; j) PPE Alu/EVA BRIDGESTONE

Minimodule consisting only of EVA and glass showed no significant changes in overall spectra after UV/T and DH exposure within 180h. On the other hand, minimodules consisting of glass/EVA/backsheets, as well as backsheets alone, showed changes in intensity of reflection around cut off region. Although changes in reflection were observed in the spectra of the backsheets, higher changes were observed in minimodules. It could be connected with permeation properties of backsheets. Acetic acid that was formed in EVA caused degradation of EVA due to longer pathway through backsheet layer, respectively. Considering behavior of EVA minimodules it can be said that backsheet layers in PV modules influenced degradation of EVA, i.e. yellowing. Also, it can be said that backsheets with higher AATR values showed lower yellowing which supports assumption that good combination of EVA and breathable backsheet are important regarding to lifetime of PV modules.

5.5. Raman spectroscopy

The Raman spectrum of an unaged minimodule EVA/glass is shown in Figure 5.16. with a detailed plot of the Raman shift area between 650 and 3250 cm^{-1}. Typical EVA peaks (cm^{-1}) of EVA at 2936 $cm^{-1}$of the symmetric stretching (v^sCH_3), at 2883 $cm^{-1}$of the CH_2 asymmetric stretching ($v^{as}CH_2$), at 2851 $cm^{-1}$of the CH_2 symmetric stretching (v^sCH_2), at 1737 $cm^{-1}$of the C=O stretching (vC=O), at 1439 $cm^{-1}$of the CH_2 scissoring (δCH_2), at 1296 $cm^{-1}$of the CH_2

twisting (tCH_2), at 1128 $cm^{-1}$and 1361 $cm^{-1}$of the C-C stretching (vC-C) could be observed. [66]

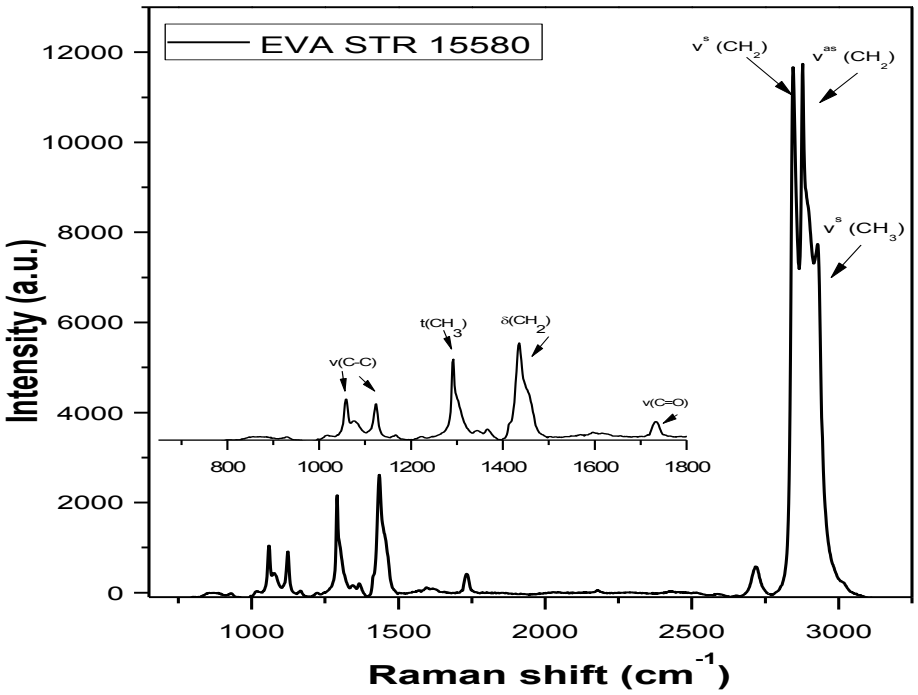

Figure 5.16. Raman spectrum of an unaged EVA minimodule

In Figure 5.17. - 5.18. the Raman spectra of EVA STR 15580, EVA BRIDGESTONE and minimodules AAA/EVA, APA/EVA, PPE/EVA and PPE Alu/EVA exposed to UV/T radiation and DH are shown. No baseline correction or normalization was made in order to show changes in baseline as consequence of fluorescence background that occurred after aging of samples.

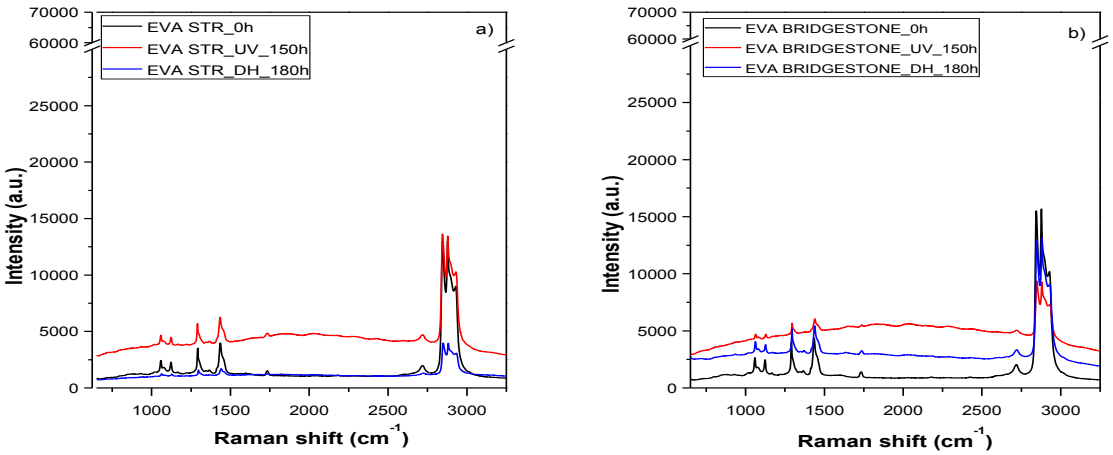

Figure 5.17. Raman spectra of unaged and aged EVA STR minimodules (a), and EVA BRIDGESTONE (b) after UV and DH exposure

It can be seen in Figure 5.17. that height of most of the most Raman peaks decreased after UV and DH exposure. Not only the height, but also the shape of Raman peaks, was influenced by the aging process, especially the shape of the CH-stretching vibrations between 2800 and 3000 cm^{-1}. It is also observed that peak at 1735 cm^{-1}which refers to carbonyl vibrations (C=O) from vinyl acetate groups decreased after aging of EVA minimodules indicating process of deacetylation. [33] No additional peaks were observed. An increase of the baseline was observed after UV/T exposure in EVA STR 15580 and EVA BRIDGESTONE, while after DH exposure no significant changes were observed in EVA STR 15580. Changes in baseline could be caused due to an increase of the fluorescence background of the material. Peike et al. described that chromophores can be formed due to material ageing that results in an increase of the fluorescence background of the material. [28,29,32] Therefore, the fluorescence intensity can be an indicator for polymer degradation since it is correlated with the amount of chromophores formed after degradation. [32,67]

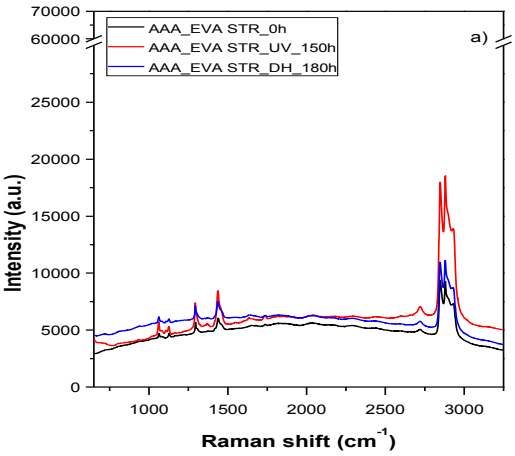
AAA_EVA STR_0h
AAA_EVA STR_UV_150h
AAA_EVA STR_DH_180h
a)
Intensity (a.u.)
Raman shift (cm-1)

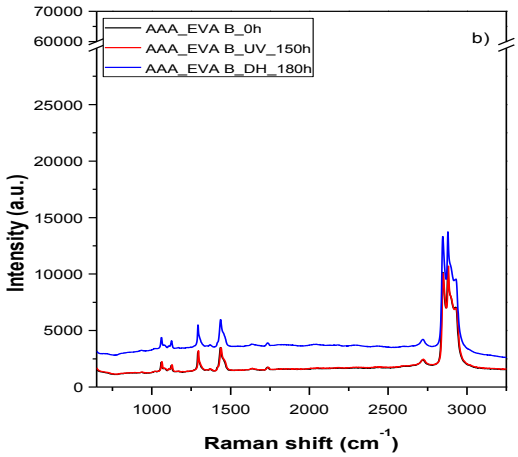
AAA_EVA B_0h
AAA_EVA B_UV_150h
AAA_EVA B_DH_180h
b)
Intensity (a.u.)
Raman shift (cm-1)

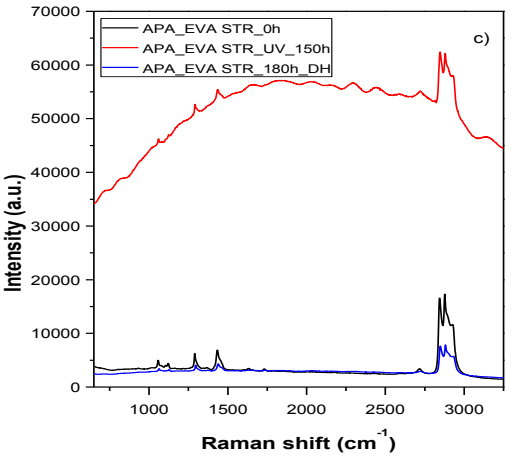
APA_EVA STR_0h
APA_EVA STR_UV_150h
APA_EVA STR_180h_DH
c)
Intensity (a.u.)
Raman shift (cm-1)

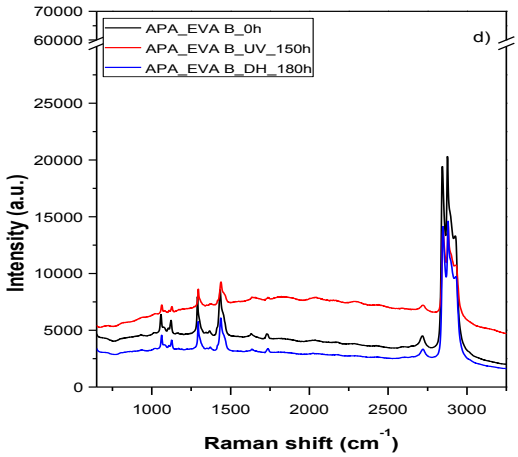
APA_EVA B_0h
APA_EVA B_UV_150h
APA_EVA B_DH_180h
d)
Intensity (a.u.)
Raman shift (cm-1)

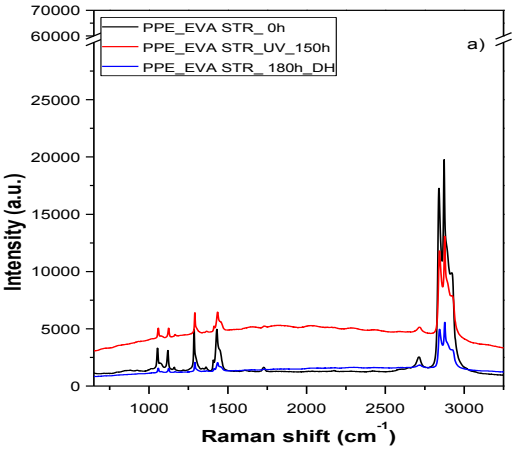
PPE_EVA STR_ 0h
PPE_EVA STR_UV_150h
PPE_EVA STR_ 180h_DH
a)
Intensity (a.u.)
Raman shift (cm-1)

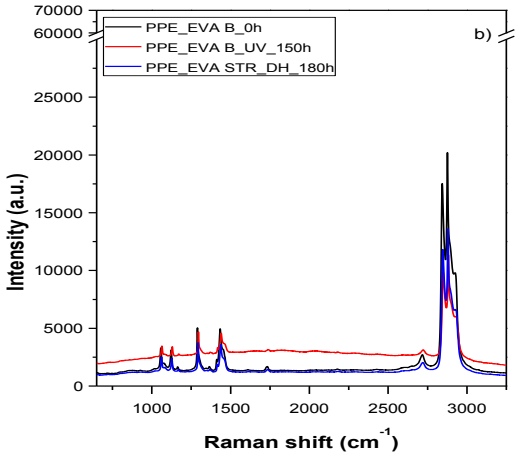
PPE_EVA B_0h
PPE_EVA B_UV_150h
PPE_EVA STR_DH_180h
b)
Intensity (a.u.)
Raman shift (cm-1)

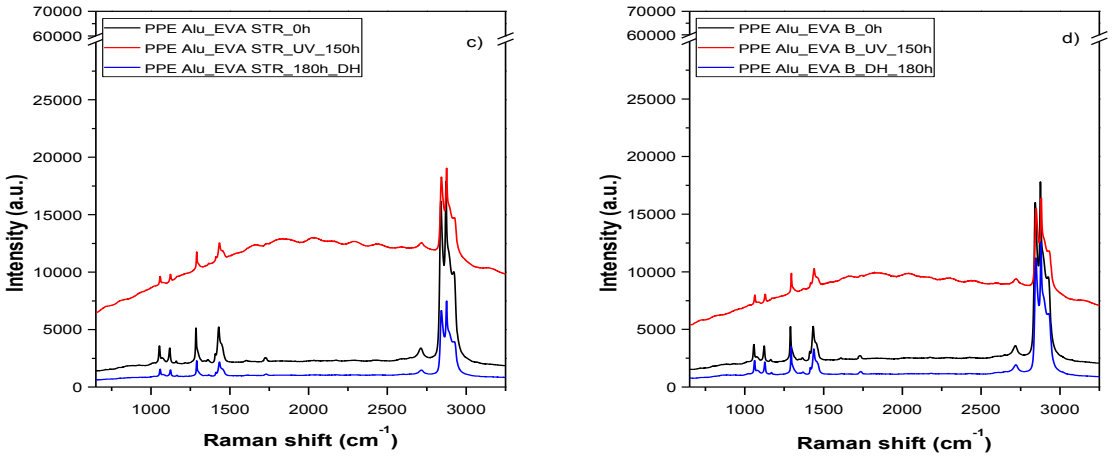

Figure 5.18. Raman spectra of the laminates with encapsulation after different aging conditions: a) AAA/EVA STR; b) AAA/EVA BRIDGESTONE; c) APA/EVA STR; d) APA/EVA BRIDGESTONE; e) PPE/EVA STR; f) PPE/EVA BRIDGESTONE; h) PPE Alu/EVA STR; i) PPE Alu/EVA BRIDGESTONE

Regarding the carbonyl peak at 1735 cm^{-1}a broadening was observed in all minimodules after aging (see Figure 5.18.). Height and shape of Raman peaks were influenced by the aging process, especially the shape of the CH-stretching vibrations between 2800 and 3000 cm^{-1}. When measured, the UV/T and DH aged minimodules exhibited an increase in the baseline, together with a decrease in relative peak intensities, due to a fluorescence background. The highest increase in baseline due to fluorescence background was observed in minimodule APA/EVA STR. It can be correlated with amount of acetic acid that was detected on the backside of minimodule APA/EVA STR in GC/MS measurements (see Figure 5.14.). Since it was assumed that acetic acid that retained at interface EVA/backsheet caused further degradation and production of acetic acid, fluorescence background in APA/EVA STR can be correlated with degradation of minimodule caused by production of acetic acid. Same baseline tendency was observed in minimodule PPE Alu/EVA STR which is also the minimodule that showed higher concentration of formed and permeated acetic acid in GC/MS measurements than other minimodules. Only slight increase in baseline is observed in AAA/EVA, which can also be correlated with amount of acetic acid detected in GC/MS measurements. This observation for AAA is in correlation with work of Peike et al. They investigated correlation between permeation properties and degradation of different encapsulation and backsheet materials where combination of EVA and PA was found to be at least affected under UV and DH conditions. [32] Also, it can be observed that minimodules combined with EVA STR 15580 showed higher increase in baseline than minimodules with EVA BRIDGESTONE.

This observation goes well with results of GC/MS measurements which showed that higher amount of acetic acid is produced in EVA STR than EVA BRIDGESTONE. A reason for that can be different formulation (additives) of EVAs.

Although higher concentration of acetic acid was found in minimodules after DH exposure (see Figure 5.14.), results of Raman spectroscopy showed that stronger influence on baseline increase had UV/T exposure than DH exposure. Hence, Raman measurements, as least obtained measurements in this work, proved assumption that permeation properties of backsheets influence degradation of PV minimodules, i.e. PV modules combined with more „breathable“ backsheets are less susceptible to degrade. Also, it is found that EVA based minimodules tend to degrade by mechanism of photodegradation more than by mechanism of thermally induced degradation.

6. Conclusions

- Thermogravimetric analysis (TGA) of EVA FC and EVA STR 15580 samples with different degree of crosslinking revealed in two steps of degradation of EVA (deacetylation and main chain cleavage) with no significant influence of degree of crosslinking on thermal stability ($T_{5\%}$, T_{1max} and T_{2max}) of EVA FC and EVA STR 15580 samples
- Acetic acid transmission rate strongly depends on temperature, film thickness, layer composition and polymer morphology (degree of crosslinking and crystallinity) and therefore transmission rates of acetic acid are lower for polymer films containing PET and/or fluoropolymer layers than for films consisting of solely polyolefines and polyamides
- Testing method with capsules in combination with GC/MS measurements is suitable for detection of permeated acetic acid on the backside of the minimodules
- "Breathable" backsheets, i.e. backsheets with high transmission rates, support diffusing out of acetic acid and right combination of EVA and backsheet can increase reliability of PV modules

7. Bibliography

[1] **Soteris, K.:** *Solar desalination systems.*., Vol. 30, Chapter 8.

[2] **Saga, T.**:*Advances in crystalline silicon solar cell technology for industrial mass production.,* NPG Asia Materials, (July 2010.), pp. 96-102

[3] **Swanson, R.-M.:** *A vision for crystalline silicon photovoltaics.*, Progress in Photovoltaics: Research and Applications, (2006.), pp. 443-453

[4] *http://iet.jrc.ec.europa.eu/remea/sites/remea/files/pv_status_report_2014_online.pdf* June, 2015.

[5] **Soteris, K.:** *Solar energy engineering: Processes and system - Photovoltaic systems* , AC Academic Press, (2013.)

[6] **Mohanty, P.; Tyagi, A.:** *Food, Energy and Water: The Chemistry Connection,* Elsevier, (2015.)

[7] **Green, M. - A.:** *Recent developments in photovoltaics,* Solar Energy, (2004.), pp. 3-8.,

[8] **Green, M. - A.:** *Consolidation of Thin-film Photovoltaic Technology: The Coming Decade of Opportunity.*, Progress in Photovoltaics: Research and Applications, (2006.), pp. 383-392.,

[9] **S.J.C.Irvine.:** *Photovoltaic (PV) thin-films for solar cells*, Woodhead Publishing Limited, (2012.), pp. 22-38,

[10] **Ferrara, C.; Philipp, D.:** *Why Do PV Modules Fail?* Energy Procedia, (2012.), pp. 379-387

[11] **Knausz, M.**: *Dissertation: Influence of Polymeric Encapsulation Materials on Quality and Reliability of PV Modules.,* Leoben , May, 2015.

[12] **King, D.L.; Quintana , M.A.; Kratochvil, J.A.; Ellibee, D.E.; Hansen, B.R.** : *Photovoltaic Module Performance and Durability Following Long-term Field Exposure.* Progress in Photovoltaics: Research and Applications, (2000.),pp. 241-256.

[13] **A.W.Czanderna; F.J.Pern.**: *Encapsulation of PV modules using ethylene vinyl acetate copolymer as a pottant: A critical review.*, Solar Energy Materials and Solar Cells, *(*1995.), pp. 101-181.

[14] **Ayutthaya, S. Isarankura Na; Wootthikanokkhan, J.:***Investigation of the Photodegradation Behaviors of an Ethylene/Vinyl Acetate Copolymer Solar Cell Encapsulant and Effects of Antioxidants on the Photostability of the Material.*, Journal of Applied Polymer Science, (2007.), pp. 3853-3863.

[15] **Hirschmann, B., Oreski, G.; Pinter, G.**: *Thermo-mechanical characterisation of fluoropolymer films for concetrated solar thermal applications.* Solar Energy Materials & Solar Cells, (2014.), pp. 615-622.

[16] **Liu, F.; Jian, L.; Yang, S.:** *UV degradation behaviour of polymeric backsheets for photovoltaic modules.*, Solar Energy, (2014.), pp. 88-100.

[17] **Gambogi, William J.:** *Comparative Performance of Backsheets for Photovoltaic Modules.,* in:25th European Photovoltaic Solar Energy Conference and Exhibition/ 5th World Conference on Photovoltaic Energy Conversion,Valencia , (2010.)

[18] **Oreski, G.; Pinter, G.:** *Aging Characterization of Multi-layer films Used as Photovoltaic Module Backsheets.* in: 28th European Photovoltaic Solar Energy Conference and Exhibition, Paris, France, (2013.)

[19] **Fu, O.; Hu, H.; Gambogi, W.-J.; Kopchick, J.-G.; Felder, T.; Babak, H.; Alex, B.; Yushi, H.; John, T.:** *Understanding backsheet durability through field studies and accelerated stress testing,* SNEC (2014.)

[20] **Knausz, M.; Oreski, G.; Eder, C.-G.; Voronko, Y.; Duscher, B.; Koch, T.; Pinter, G.; Berger, K.-A.:***Degradation of photovoltaic backsheets: Comparison of the aging induced changes on module and component level.*, Journal of Applied Polymer Science, (2015.)

[21] **Oreski, G.; Wallner, G.M.**: *Aging mechanisms of polymeric films for PV encapsulation.* Solar Energy, (2005.), pp. 612-617.

[22] **Skoczek, A.; Sample, T.; Dunlop, E.D.:***The Results of Performance Measurements of Field-aged Crystalline Silicon Photovoltaic Modules.*, Progress in Photovoltaics: Research and Applications, (2009.), pp. 227-240.

[23] **B. Lalaguna, P. Sánchez-Friera, F. Ropero, J. F. Gil, J. Alonso.:** *Comparison of Moisture Ingress in PV Modules wih Different Backsheets Using Humidity Sensors.* In: 23rd European Photovoltaic Solae Energy Conference,Valencia, 2008.

[24] **Harper, C.A.:** *Modern Plastics Handbook,* Technology seminars, Inc.

[25] **Kempe, M.D.; Jorgensen, G.J.; Terwilliger, K.M.; McMahon, T.J.; Kennedy, C.E.; Borek, T.T.:** *Acetic acid production and glass transitions concerns with ethylene-vinyl acetate used in photovoltaic devices*, Solar Energy Materials and Solar Cells,(2007.), pp. 315-329.

[26] **Jing, J., Chen, S.; Zhang, J.:** *UV aging behaviour of ethylene-vinyl acetate copolymers (EVA) eith different vinyl acetate contents,* Polymer Degradation and Stability, (2010.), pp. 725-732.

[27] **Peike, C.; Kaltenbach, T.; Koehl, M.; Weiss, K.-A.:** *Lateral distribution of the degradation of encapsulants after different damp-heat exposure times investigated by Raman spectroscopy,* Proc. Of SPIE Vol. 7773, *(* 2010.)

[28] **Peike, C.; Kaltenbach, T.; Weiss, K.-A.; Koehl, M.:** *Non-destructive degradation analysis of encapsulants in PV modules by Raman Spectroscopy*, Solar Energy Materials & Solar Cells, (2011.), pp. 1686-1693.

[29] **Peike, C.; Purschke, L.; Weiss, K.-A-; Koehl, M.; Kempe, M.:** *Towards the origin of photochemical EVA discoloration.* In: 39th Photovoltaic Specialists Conference IEEE,Tampa Bay, USA, (2013.)

[30] **Allen, N.S., Edge, M., Rodgriuez, M.:** *Aspects of the thermal oxidation, yellowing and stabilisation of ethylene vinyl acetate copolymer,* Polymer Degradation and Stability 71, (2001.), pp. 1-14

[31] **Schlothauer, J., Jungwirth, S., Köhl, M., Röder, B.:** *Degradation of the encapsulant polymer in outdoor weathered photovoltaic modules: Spatially resolved inspection of EVA ageing by fluorescence and correaltion to electroluminescence,* Solar Energy Materials & Solar cells 102, (2012.), pp. 75-85.

[32] **Peike, C.,Huelsmann, P.; Blueml, M.; Schmid, P.; Weiss, K.-A.; Koehl, M.:** *The impact of permeation properties and backsheet-encapsulant interactions on the reliability of PV modules.* (2012.), Article ID 459731.

[33] **Beinert, A.; Peike, C.; Duerr, I.; Kempe, M.; Weiss, K.A.:** *The influence of the aditive composition on degradation induced changes in poly (ethylene-co-vinyl acetate) during photochemical aging,* In: 29th European PV Solar Energy Conference and Exhibition,Amsterdam, (2014.)

[34] **Sample, T***: Failure modes observed in real use and long-term exposure,* In: PV Module Reliability Workshop, Berlin, Germany, (2011.)

[35] **Wagner ,F.**: Master thesis: *Characterisation of Chemical Ageing Processes in Encapsulant Materials Used in PV Modules.* May, (2015.), PCCL, Leoben .

[36] **Klemchuk, P.; Ezrin, E.; Lavigne, G.; Holley, W.; Galica, J.; Agro, S.:** *Investigation of the degradation and stabilization of EVA-based encapsulants in field-aged solar energy modules*, Polymer Degradation and Stability, (1997.), pp. 347-365.

[37] **L.-E. Perret-Aebi, H.-Y. Li, R. Théron, G. Roeder, Y. Luo, T. Turlings, R. F. M. Lange, C. Ballif:** *Insight on EVA lamination process: Where do the bubbles come from?*, in: 25th European Photovoltaic Solar Energy Conference and Exhibition, Valencia, Spain, (2010.)

[38] **Zamini, Krametz et al.***: " Reliability, characterization, and performance of photovoltaic modules",* Elektrotech. Inftech. (e & i Elektrotechnik und Informationstechnik), 126 volume, 9 issue, (2009.), pp. 335-339.

[39] **Weber, U., et al.:** *Acetic acid production, migration and corrosion effects in ethylene-vinyl-acetate-(EVA) based PV modules.* In: 27th European Photovoltaic Solar Energy Conference and Exhibition, pp. 2992-2995.

[40] **Ketola, B.; Norris, A.:** *The role of encapsulant moisture permeability in the durability of solar photovoltaic modules,* in: 25th European Photovoltaic Solar Energy Conference and Exhibition/ 5th World Conference on Photovoltaic Energy Conversion, 6-10 September 2010, Valencia, Spain

[41] **Mark, H.F.:***"Barrier Polymers", In: Encyclopedia of Polymer Science and Technology, 5th ed.* New York : John Wiley & Sons Inc., (2002.)

[42] **D.W.vanKrevelen; Nijenhuis, K.**: *Properties of polymers: Their Correlation with Chemical Structure; their Numerical Estimation and Prediction from Additive Group Contributions,* Elsevier, (2009.)

[43] **Duncan, B.; Urquhart, J.; Roberts, S.:** *Review of Measurement and Modelling of Permeation and Diffusion in Polymers,* NPL Report DEPC MPR 012, (2005.)

[44] **Massey, L.-K.:** *Permeability properties of plastics and elastomers, 2nd edition: A guide to packaging and barrier materials*, Plastics Design Library, (2003.)

[45] **Hülsmann, P.; Phillip, D.; Koehl, M.:** *Measuring temperature dependant water vapor and gas permeation through high barrier films*, Review of Scientific Instruments 80, (2009.), 113901-1-6

[46] http://www.upcinc.com/, May, 2015.

[47] **D., Yao, Qu, B.; Wu, Q.:***Photoinitiated Crosslinking of Ethylene-Vinyl Acetate Copolymers and Characterization of Related Properties*, Polymer Engineering and Science, (2007.), pp. 1761-1767.

[48] **Soudais, Y.; Moga, L.; Blazek, J.; Lemort, F.:** *Coupled DTA-TGA- FT-IR investigation of pyrolytic decomposition of EVA, PVC and cellulose*, Journal of Analytical and Applied Pyrolysis, (2007.), pp. 46-57.

[49] **Hirschl, C.,Neumaier, L.; Muehleisen, W.; DeBiasio, M.; Oreski, G.; Rauschenbach, A.; Eder, G.; Chernev, B.S.; Kraft, M.:** *Post-crosslinking in PV modules under different conditions,* in: 29th European Photovoltaic Solar Energy Conference and Exhibition, Amsterdam, Netherlands, (2014.)

[50] **Hirschl, C.; Biebl – Rydlo, M.; DeBiasio, M.; Muehleisen, W.; Neumaier, L.; Scherf, W.; Oreski, G.; Eder, G.; Chernev, B.S.; Schwab, W.; Kraft, M.:** *Determining the degree of crosslinking of ethylene vinyl acetate photovoltaic module encapsulants - A comparative study* Solar Energy Materials & Solar Cells, (2013.), pp. 203-218.

[51] **M.D.Kempe:** *Ultraviolet light test and evaluation methods for enacpsulants of PV modules*, Solar Energy Materials and Solar Cells, (2010.), pp. 246-253.

[52] **Prime R.-B.; Bair E.-H.; Vyazovkin S.; Gallagher P.-K.; Riga A.:** "*Thermal Analysis of Polymers - Fundamentals and Applications*", A John Wiley & Sons, INC., Publication, (2009.)

[53] http://radchem.nevada.edu/, June, 2015.

[54] *http://pubs.rsc.org/en/content/articlehtml/2014/ta/c3ta13779a,* June, 2015.

[55] **Mihaljevic, A.:** *The Effect of SEBS block copolymer as a compatibilizer on application properties of TPU/PP blends,* Zagreb, FKIT, (2014.)

[56] *http://konmarklab.hr/metode-rada/,* July, 2015.

[57] *https://en.wikipedia.org/wiki/Gas_chromatography%E2%80%93mass_spectrometry,* July, 2015.

[58] *http://www.perkinelmer.com/,* July, 2015.

[59] **Planes, E.; Yrieix, B.; Bas, C.; Flandin, l.:** *Chemical degradation of the encapsulation system in flexible PV panel as revealed by infrared and Raman microscopies,* Solar Eneergy Materials & Solar Cells, (2014.), pp. 15-23.

[60] **Lin-Vien, Daimay***: Infrared and Raman Characteristic Frequencies of Organic Molecules,* Academic Press Boston, (1991.)

[61] **Jacobsson, P.; Johansson, P.:** *Vibrational Properties: Raman and Infra Red.,* Elsevier B.V., (2009.)

[62] . **Schrader, B.:** *IR and Raman Spectroscopy*, Wiley-VCH, Weinheim, Germany , (1995.)

[63] *http://www.americanpharmaceuticalreview.com/* June, 2015.

[64] . **Vazquez-Rodriguez, M.; Liauw, C.-M.; Allen, N.-S.; Edge, M.; Fontan, E.**: *Degradation and stabilisation of poly(ethylene-stat-vinyl acetate): 1-Spectroscopic and rheological examination of thermal and thermo-oxidative degradation mechanisams*, Polymer Degradation and Stability, (2006.), pp. 156-164.

[65] http://www.solvayplastics.com/, August, 2015.

[66] **Shimoyama, M.; Maeda, H.; Matskuawa, K.; Inoue, H.; Ninomya, T.; Ozaki, Y.**:*Vibrational Spectroscopy 14.*, (1997.)

[67] **Lee, Y.-H., Li, Y.-T.; Wang, B.-F.; Lin, Y.-W.; Wu, H.-S.; Huang, D.-R.:** *A novel approach to yellowing process and formation of chromophores in EVA sheets by two UV-aging methods,* In: 29th European Photovoltaic Solar Energy Conference and Exhibition. pp. 140-142.

8. Biography

I was born in Split on 15.12.1991.. Primary and high school I ended in Vrgorac. In 2013. I enrolled undergraduate study programme Chemical Technology on Faculty of Chemistry and Technology at University of Split and decided to proceed with my further education in Zagreb at Faculty of Chemical Engineering and Technology at University of Zagreb, where I enrolled graduate study programme Materials Science and Engineering. In 2014. I was doing an internship programme in Leoben (Austria) in Polymer Compentence Center Leoben (PCCL) within the project Bio4Sun „Biogene Kunststoffe für solartechnische Applikationen“. In 2014. I won rectors prize for scientific work “The Effect of SEBS block copolymer as a compatibilizer on application properties of TPU/PP blends”. In 2015. I got national scholarship for the best students at University of Zagreb in year 2013./2014.